ANL/NDM-2

PROMPT AIR-SCATTERING CORRECTIONS FOR A FAST-NEUTRON FISSION DETECTOR: $E_n \leq 5$ MeV

by

Donald L. Smith

September 1973

NOTICE

This report was prepared as an account of work sponsored by the United States Government. Neither the United States nor the United States Atomic Energy Commission, nor any of their employees, nor any of their contractors, subcontractors, or their employees, makes any warranty, express or implied, or assumes any legal liability or responsibility for the accuracy, completeness or usefulness of any information, apparatus, product or process disclosed, or represents that its use would not infringe privately owned rights.

Applied Physics Division
Argonne National Laboratory
9700 South Cass Avenue
Argonne, Illinois 60439
U.S.A.

DISTRIBUTION OF THIS DOCUMENT IS UNLIMITED

NUCLEAR DATA AND MEASUREMENTS SERIES

The Nuclear Data and Measurements Series presents results of studies in the field of microscopic nuclear data. The primary objective is the dissemination of information in the comprehensive form required for nuclear technology applications. This Series is devoted to: a) Measured microscopic nuclear parameters, b) Experimental techniques and facilities employed in data measurements, c) The analysis, correlation and interpretation of nuclear data, and d) The evaluation of nuclear data. Contributions to this Series are reviewed to assure a high technical excellence and, unless otherwise stated, the contents can be formally referenced. This Series does not surplant formal journal publication but it does provide the more extensive information required for technological applications (e.g. tabulated numerical data) in a timely manner.

TABLE OF CONTENTS

	Page
ABSTRACT	3
I. INTRODUCTION	4
II. PHYSICAL PROPERTIES OF AIR	5
III. SIMPLE ANALYTIC FORMULATION	7
IV. ISOTROPIC SINGLE ELASTIC - SCATTERING FORMULATION	10
V. DETAILED SINGLE-SCATTERING FORMULATION	15
VI. CONCLUSIONS	20
ACKNOWLEDGEMENTS	21
APPENDIX I: Listing of FORTRAN IV Code-AIRSC1	63
APPENDIX II: Listing of FORTRAN IV Code-AIRSC2	69

PROMPT AIR-SCATTERING CORRECTIONS FOR A FAST-NEUTRON FISSION DETECTOR: $E_n \lesssim 5$ MeV

by

Donald L. Smith

ABSTRACT

Neutrons which have scattered many times in surrounding air and in laboratory objects arrive randomly in time at a detector and can be discriminated by time-of-flight techniques. Neutrons which have scattered only a few times in air reach the detector soon after the primary neutron burst and cannot be distinguished from the latter by time conditions. Most of the prompt air-scattered neutrons have undergone only one elastic collision and it has been shown that the ratio of these singly-scattered to primary neutrons increases linearly with distance from a point source. The energy, time and angular distributions of neutrons which scatter once in surrounding air before reaching a fission detector have been calculated for E_n = 0.05 - 5 MeV using published cross sections. Data corrections for prompt air-scattered neutrons are generally small but not necessarily negligible in high-precision measurements. For example, it has been calculated that this effect leads to a correction of $\sim$ 0.2 - 0.3% in a measurement at E_n = 1.5 MeV of the U-238 to U-235 fission cross section ratio if the back-to-back uranium deposits in a double fission detector are situated 10 cm from the neutron source. This correction is significant since $\lesssim$ 1% accuracy is currently sought in fission cross section ratio measurements.

I. INTRODUCTION

We shall consider a predominantly fast-neutron field whose source is for practical purposes a point (e.g. bombardment of a lithium target with a focused proton beam from an accelerator). The neutron field at an arbitrarily distant observation point is composed of primary neutrons and of neutrons which have scattered in surrounding air and in laboratory objects. The response of a fission detector to these neutrons depends upon the isotopic constituency of the fissionable material in the detector as well as on the characteristics of the field.

Air is a rather sparse medium and the ratio of air-scattered to primary flux is generally small unless the observation point is relatively far from the source. One of the best ways to minimize the influence of air scattering in an experiment is to choose an irradiation position which is as close to the source as possible. Another approach which may be employed to minimize external scattering problems is to irradiate samples and a monitor in the same geometry. External scattering corrections tend to cancel for these relative measurements unless the cross sections involved vary considerably with energy.

Multiple scattering eventually generates a thermal neutron background with weak spatial variation in the vicinity of the source. Thermal neutrons can be extremely troublesome for a fission detector containing a deposit enriched in an isotope with a large thermal fission cross section. Fortunately, time-of-flight techniques can be utilized to reject thermal background in many fast-neutron experiments. Otherwise, it is necessary to place the fission detector close enough to the source so that the thermal correction is manageably small. Hydrogenous laboratory materials such as water, paraffin and concrete are very effective in thermalizing neutrons. Surrounding air and non-hydrogenous laboratory materials also contribute to thermalization. Since experimental techniques exist for minimizing

the effects of thermal neutrons in most fast-neutron experiments, this topic will not be considered further in this paper.

Neutrons which scatter only a few times in air in the vicinity of the source and lose only part of their primary energy can produce fissions and hence cannot be distinguished from primary-neutron fissions by time-of-flight. One could minimize this problem by placing the detector very close to the source, but this is not always feasible. It is the influence of these prompt air-scattered neutrons which has been investigated in the present work. The term "air-scattered neutrons" as used in the remainder of this report implies prompt air-scattered neutrons.

For a monoenergetic point neutron source, define:

(r,θ) = polar coordinates of the observation point with the source situated at the origin. Air scattering exhibits no azimuthal dependence in a homogeneous medium.

$\Sigma_{T,AIR}$ = macroscopic neutron total cross section for air.

$f_o(\theta)/r^2$ = vacuum flux (neutrons/cm^2 / sec).

$f(r,\theta)/r^2$ = true flux at the observation point (neutrons/cm^2/sec).

$F(r,\theta)$ = relative intensity of air-scattered and direct neutrons at the observation point.

Then

$$f\ (r,\theta) = f_o\ (\theta)\ [1 + F(r,\theta)]\ \exp(-r\Sigma_{T,AIR}). \qquad (1)$$

Eq. (1) provides no information about the energies, arrival times and angles of incidence for scattered neutrons reaching the detector. These factors along with properties of the detector determine the relationship between the observed detector response and the neutron field which is to be measured.

II. PHYSICAL PROPERTIES OF AIR

For the present analysis, dry air is represented by a mixture of nitrogen (79.1%) and oxygen (20.9%) with a total density of 1.205 x

10^{-3} grams per cm^3 under normal conditions (temperature = 20°C and pressure = 76 cm Hg) [1]. The only isotopes of nitrogen and oxygen which are significant are N-14 (99.63% of natural nitrogen and 0-16 (99.759% of natural oxygen) [2]. The atomic densities of these isotopes are 4.034×10^{19} atoms of N-14 and 1.066×10^{19} atoms of 0-16 per cm^3 of air. The concentrations of the rare gases (argon, etc.) are too small to significantly affect the neutron scattering properties of air. The H_2O vapor content of air is variable, but amounts to 1.7118×10^{-5} grams per cm^3 of air for 20°C at the saturation level [1]. This corresponds to 1.145×10^{18} atoms of hydrogen and 5.724×10^{17} atoms of oxygen per cm^3 of air. The presence of hydrogen in H_2O vapor is likely to have a noticeable effect on the thermalization of neutrons emitted from the source. On the other hand, the H_2O vapor is unlikely to have much influence on the fast-neutron scattering properties of air (except possibly near the oxygen resonance at 0.44 MeV) and therefore, H_2O vapor will be ignored in the present work.

For $E_n \lesssim 5$ MeV, neutron scattering by N-14 proceeds predominantly via elastic scattering with a small contribution from inelastic scattering through the 3.945 MeV excited state. All scattering from 0-16 is elastic for $E_n < 6.13$ MeV. Total, elastic scattering and inelastic scattering cross sections from an evaluation by J. H. Ray et al. [3] have been used in the present work. Selected cross section values from this reference are listed in Table I (nitrogen) and Table II (oxygen).

Inelastic scattering from nitrogen is assumed to be isotropic in the laboratory. Tables of Legendre coefficients for nitrogen and oxygen elastic scattering angular distributions are given as a function of neutron energy in Ref. 3. These distributions refer to the center-of-mass system and are presented in the form:

$$\frac{d\sigma_E}{d\Omega}\Big|_{CM}(\theta_{CM}) = (\sigma_E/4\pi)\ [\ 1 + \sum_{k=1}^{n} (2k + 1)\ f_k P_k(\cos\theta_{CM})\ ] \qquad (2)$$

where P_k $(\cos\Theta_{CM})$ is a Legendre polynomial of order k. The center-of-mass system angular distributions from Ref. 3 were transformed to the laboratory system for use in the present work. Sets of coefficients (w_k) were generated where

$$\left.\frac{d\sigma_E}{d\Omega}\right|_{LAB} (\Theta_{LAB}) = (\sigma_E/4\pi)[\,1 + \sum_{k=1}^{m} w_k P_k\,(\cos\Theta_{LAB})]. \qquad (3)$$

The shapes of the laboratory elastic-scattering angular distributions were reproduced quite well at all energies by using fifth-order expansions (m=5). Sets of coefficients $\{w_k\}$ for various neutron energies are given in Table III (nitrogen) and Table IV (oxygen). Plots of the elastic-scattering angular distributions for selected neutron energies appear in Fig. 1 (nitrogen) and Fig. 2 (oxygen).

III. SIMPLE ANALYTIC FORMULATION

The analysis in this report assumes a detector which is essentially a parallel-plate ionization chamber with a thin film of fissionable material in the form of a circular disk deposited on one of the plates [4]. Fig. 3 is a schematic diagram which shows the relationship of the fissionable deposit and the point neutron source and defines several geometrical parameters required for calculations. Scattering by other components of the fission chamber constitutes a separate problem which will not be considered here.

It is not hard to derive an expression for the relative intensity of the singly-scattered neutrons to the primary neutrons at the center of the deposit [coordinates (0,0,0) in Fig. 3] if the following approximations are made:

a. Emission from the source is monoenergetic and isotropic.
b. Energy loss by neutrons in elastic scattering from nitrogen or oxygen is ignored.
c. Neutron scattering by nitrogen or oxygen is isotropic in the laboratory.
d. Flux attenuation along the propagation paths is neglected.

Let

F_0 = relative intensity of singly-scattered neutrons to the primary neutrons as computed by the method described in this section.

Then

$$F_0 = (\Sigma_{E,AIR} d^2/4\pi) \int_{\substack{ALL \\ SPACE}} (1/d_2^2)\ \delta d_1 \delta\Omega_{S1} \tag{4}$$

where

$\Sigma_{E,AIR}$ = macroscopic neutron elastic scattering cross section for air

and values for d_1 and d_2 as defined in Fig. 3 are computed for r_F = 0 (θ_{S0} = 0).

Azimuthal symmetry and the law of cosines may be applied to obtain the formulas

$$d_2^2 = d^2 + d_1^2 - 2d\ d_1 \cos\theta_{S1} \tag{5}$$

and

$$F_0 = (\Sigma_{E,AIR} d^2/2) \int_0^\infty \delta d_1 \int_0^\pi \delta\theta_{S1} \sin\theta_{S1} \quad X$$
$$X \quad (d^2 + d_1^2 - 2\ d\ d_1 \cos\theta_{S1})^{-1}. \tag{6}$$

A change of variables and partial integra ion yields the expression

$$F_0 = (\Sigma_{E,AIR} d\ /2) \int_0^\infty \frac{\delta X}{X}\ \ln\left(\frac{1+X}{1-X}\right). \tag{7}$$

From integral tables in Ref. 1 one obtains

$$\int_0^\infty \frac{\delta X}{X}\ \ln\left(\frac{1+X}{1-X}\right) = 2\int_0^1 \frac{\delta X}{X}\ \ln\left(\frac{1+X}{1-X}\right) = \frac{\pi^2}{2} \tag{8}$$

and consequently

$$F_0 = (\pi^2\ \Sigma_{E,AIR} d/4). \tag{9}$$

The mean free path for elastic scattering λ_E is defined to be the reciprocal of the macroscopic elastic scattering cross section $\Sigma_{E,AIR}$, therefore

$$F_0 \approx 2.47\ (d/\lambda_E). \tag{10}$$

The interpretation of Eq. (8) is that half of the air-scattered neutrons originate from within a sphere of radius d centered at the neutron source while the rest of the scattered neutrons come from all space exterior to this sphere. The mean free path for elastic scattering in air can be computed from the formula

$$\lambda_E = [\ (4.034 \times 10^{-5})\ \sigma_{E,N} + (1.066 \times 10^{-5})\ \sigma_{E,O}]^{-1} \qquad (11)$$

using cross section values in barns from Tables I and II (see Section II). Values of λ_E computed from Eq. (11) appear in Table V. The solid curve in Fig. 4 is a plot of F_0 computed with Eq. (10) and values of λ_E from Table V for d = 5 cm. Notice the effect of the oxygen scattering resonance at E_n = 0.44 MeV.

Only singly-scattered neutrons were considered in the preceding analysis. A rudimentary argument for neglecting higher-order scattering will now be presented. Let us assume that time-of-flight conditions preclude detection of any neutron which has propagated along a path (not necessarily in a straight line) of length exceeding L. By definition of the mean free path λ_E, the average number of collisions experienced by a neutron along a path of length L is L/λ_E. The probability of the neutron experiencing exactly N collisions is given by the Poisson distribution

$$P_N = (L/\lambda_E)^N e^{-L/\lambda_E} /N! \qquad (12)$$

From Eq. (12) it is seen that the probability of zero collisions P_0 is e^{-L/λ_E} which is exactly what one would expect since e^{-L/λ_E} is the attenuation coefficient. The probability of experiencing any sort of collision (without specifying the order) is just $(1-e^{-L/\lambda_E})$. The probability P_1 of a single collision is $(L/\lambda_E)\ e^{-L/\lambda_E}$ and, in general, the ratio of P_N to P_{N-1} is simply $(L/N\lambda_E)$. From Table V it is seen that λ_E = 6854 cm for E_n = 1 MeV. On the other hand, a reasonable time limitation imposed by time-of-flight discrimination would be ∿ 20 nanoseconds. This implies L = 277 cm and a corresponding ratio of P_2 to P_1 of ∿ 0.02. Higher orders of scattering are

even more negligible.

Langsdorf has shown by means of an analysis resembling that which led to Eq. (9) that the ratio of doubly air-scattered neutrons to primary neutrons can be approximated by a relatively simple formula for small values of d/λ_E [5]. Application of this formula for E_n = 1 MeV and d = 5 cm yields a ratio of $\sim 10^{-5}$ for doubly scattered to primary neutrons and $\sim$0.006 for the ratio of doubly scattered to singly scattered neutrons. This result indicates that the rudimentary approach discussed in the preceding paragraph may overestimate the importance of higher-order scattering. Consequently, only single scattering will be considered for the remainder of this report.

IV. ISOTROPIC SINGLE ELASTIC-SCATTERING FORMULATION

The relative intensity of scattered and primary neutrons can be estimated easily from Eqs. (10) and (11). The only additional piece of information which the formulation in Section III provides is that half of the air-scattered flux originates from within a distance d of the source. A different approach is required to study the effects of finite detector size and to determine the incidence-angle and arrival-time distributions for air-scattered neutrons. These additional aspects will be investigated in the present section within the framework of the approximations stated in Section III.

The appropriate geometry for the following analysis is shown in Fig. 3. It is advantageous to define a set of cylindrical coordinates (r_A, ϕ_A, Z_A) with origin (0,0,0) at the center of the uranium deposit. The point neutron source is situated on the axis at coordinates (0,0,d). The uranium deposit is taken to be a very thin circular disk with radius R_{DISK}. Let

F_1 = relative number of air-scattered neutrons to primary neutrons incident upon the deposit as computed by the method described in this section.

then

$$F_1 = (\Sigma_{E,AIR}/4\pi)\frac{\left[\int_0^{R_{DISK}} \delta r_F \int_0^{\infty} \delta r_A \int_{-\infty}^{\infty} \delta Z_A \int_0^{2\pi} \delta\phi_A \mathcal{G}(d,r_F,r_A,Z_A,\phi_A)\right]}{\left[\int_0^{R_{DISK}} \delta r_F \mathcal{F}(d,r_F)\right]} \quad (13)$$

where

$$\mathcal{F}(d,r_F) = r_F/(r_F^2 + d^2) \quad (14)$$

$$\mathcal{G}(d,r_F,r_A,Z_A,\phi_A) = (r_A r_F/d_1^2 d_2^2) \quad (15)$$

$$d_1^2 = X_A^2 + Y_A^2 + (Z_A - d)^2 \quad (16)$$

$$d_2^2 = (X_A - r_F)^2 + Y_A^2 + Z_A^2 \quad (17)$$

The indicated integration of Eq. (13) extends over the surface of the disk and over all air space. Since most of the air-scattered neutrons come from the vicinity of the source, it is reasonable to set limits on the region of air space included in the evaluation of F_1. Thus

$$F_1 \approx (\Sigma_{E,AIR}/4\pi)\frac{\left[\int_0^{R_{DISK}} \delta r_F \int_0^{R_{A,MAX}} \delta r_A \int_{-Z_{A,MAX}}^{+Z_{A,MAX}} \int_0^{2\pi} \delta\phi_A \mathcal{G}(d,r_F,Z_A,\phi_A)\right]}{\left[\int_0^{R_{DISK}} \delta r_F \mathcal{F}(d,r_F)\right]} \quad (18)$$

where $R_{A,MAX}$ and $Z_{A,MAX}$ are limits on the coordinates r_A and Z_A which define a pillbox surrounding the uranium deposit. The integrals appearing in Eq. (18) are evaluated by a Monte-Carlo technique. The expression

$$F_1 \approx \Sigma_{E,AIR}\, R_{A,MAX}\, Z_{A,MAX} \frac{\left[\left(\sum_{j=1}^{N_{HIST}} \mathcal{G}_j\right)/N_{HIST}\right]}{\left[\left(\sum_{j=1}^{M_{HIST}} \mathcal{F}_j\right)/M_{HIST}\right]} \quad (19)$$

is an approximation to Eq. (18) which improves in accuracy with increased numbers N_{HIST} and M_{HIST} of sampling histories. (M_{HIST} can

be considerably smaller than N_{HIST}). Choice of values for M_{HIST} and N_{HIST} is a matter of compromise between computational time and statistical stability. Random values for r_F, r_A, Z_A and ϕ_A were computed for each history from the equations

$$r_F = R_{DISK}\, \eta_F \quad (0 < \eta_F \leq 1) \tag{20}$$

$$r_F = R_{A,MAX}\, \eta_R (0 < \eta_R \leq 1) \tag{21}$$

$$Z_A = -Z_{A,MAX} + 2Z_{A,MAX}\eta_Z \tag{22}$$

$$(0 < \eta_Z \leq 1)$$

$$\phi_A = 2\pi\eta_\phi \quad (0 < \eta_\phi \leq 1) \tag{23}$$

where η_F, η_R, η_Z and η_ϕ are random numbers.

An advantage of this method is that it permits one to easily calculate distributions and history averages of other parameters using the same weighting factors $\mathcal{F}_j$ and $\mathcal{G}_j$ from Eqs. (14) and (15). The arrival-time distribution for air-scattered neutrons is of interest for time-of-flight applications because one wishes to know to what extent the air-scattered neutrons straggle with respect to the primary neutrons and thereby produce a "late-arrival" tail on the time peak generated by a pulsed neutron source. The minimum flight time from the neutron source to the uranium disk is given by

$$T_{MIN} = d/v_n \tag{24}$$

where

v_n = velocity of the neutrons

and this corresponds to propagation along the axis. The longest flight time for primary neutrons is given by

$$T_{MAX} = (d^2 + R_{DISK}^2)^{\frac{1}{2}}/v_n \tag{25}$$

and $(T_{MAX} - T_{MIN})$ is usually smaller than the experimental time resolution. The flight time for an air-scattered neutron (with no energy loss) is given by

$$T = (d_1 + d_2)/v_n \tag{26}$$

which could be significant if $(d_1 + d_2) >> d$. During the process of evaluating the numerator of Eq. (19) one can compute flight times T_j, each weighted by the appropriate value $\mathcal{Y}_j$, and thereby generate a time distribution. In the present work, the time interval $(0, T_{RANG})$ was divided into N_{TIME} equal time intervals. If the following inequality

$$[(k-1)T_{RANG}/N_{TIME}] \leq (T_j - T_{MIN}) \leq [k\, T_{RANG}/N_{TIME}] \qquad (27)$$

is satisfied for the jth history, then $\mathcal{Y}_j$ is added to the weight factor $\mathcal{Z}_k$ for the kth "bin" of the discrete time distribution function. The collection of values $\{\mathcal{Z}_k\}$ obtained from following N_{HIST} histories defines the unnormalized time distribution function. Contributions from histories for which $(T_j - T_{MIN})$ exceed T_{RANG} are recorded in an "overflow" bin. Use of such an "overflow" bin permits one to calculate how many events will be lost as a result of air scattering when a "window" is placed on the time peak during a measurement.

The angle of incidence Θ_I for neutrons which scatter from air in the vicinity of the point (X_A, Y_A, Z_A) and subsequently reach the uranium deposit at the point $(r_F, 0, 0)$ can be calculated by analytic geometry (see Fig. 3). The angle-of-incidence distribution function and the history average $\bar{\Theta}_I$ can be computed in a manner similar to that used for obtaining the arrival-time distribution function. The angle-of-incidence distribution function is a useful aid in understanding the air-scattering problem because it indicates the direction from which most of the air-scattered neutrons impinge on the uranium deposit.

Calculations were made on a digital computer using the formalism described in the preceding paragraphs. See Appendix I for a listing of the FORTRAN IV code AIRSC1 which was written to perform these calculations. The values $M_{HIST} = 2000$ and $N_{HIST} = 20000$ were found to yield sufficient statistical stability for the present work. Values of F_1 computed from Eq. (13) should approximate corresponding values of F_0 from Eq. (10)--if finite uranium deposit size effects are neglected--since both formulations of the problem are based on

the same set of physical assumptions. To test this point and to determine how large $R_{A,MAX}$ and $Z_{A,MAX}$ have to be so that Eq. (18) becomes a good approximation to Eq. (13) the following two sets of calculations were made:

a. The ratio F_1/F_0 was computed for several values of $R_{A,MAX}$ (= $Z_{A,MAX}$) with E_n = 1 MeV, R_{DISK} = 1.27 cm and d = 5 cm.
b. The ratio F_1/F_0 was computed for several values of d with E_n = 1 MeV, R_{DISK} = 1.27 cm and $R_{A,MAX} = Z_{A,MAX} \geq 10$ d.

The results of these sets of calculations appear in Figs. 5 - 8. From the values of F_1/F_0 plotted in Fig. 5 one can conclude that about half of the air-scattered flux originates from the region of air space for which $R_{A,MAX} = Z_{A,MAX} \lesssim$ d which is in agreement with the interpretation of Eq. (8). From Fig. 6 it is evident that the effects of the finite size of the uranium deposit essentially disappear for $d/R_{DISK} > 3$. This fact can also be deduced from Fig. 7 which is a plot of $\bar{\theta}_I$ vs. d/R_{DISK}. $\bar{\theta}_I$ approaches a limit of $\sim 60°$ for $d/R_{DISK} > 3$. The variation in shape of the angle-of-incidence distribution functions with d/R_{DISK} is shown in Fig. 8. The effect of finite uranium deposit size is to produce a forward-angle dip in the distribution function. This structural feature is still evident for $d/R_{DISK} \sim 5$. However, for larger values of d/R_{DISK} this feature disappears and the distribution function becomes approximately linear in $\bar{\theta}_I$.

Another set of calculations was made for various neutron energies with R_{DISK} = 1.27 cm, d = 5 cm (d/R_{DISK} = 3.94) and $R_{A,MAX} = Z_{A,MAX} > 10$ d. The resulting values of F_1 are plotted in Fig. 4. Except for some statistical fluctuation, the values of F_0 and F_1 are in excellent agreement. Corresponding scattered neutron arrival-time distributions were obtained from the same set of calculations and these appear in Fig. 9. Notice that even for low energies most of the scattered neutrons arrive at the uranium deposit within a few nanoseconds after the primary neutrons. It is clear that it is not feasible to eliminate the effects of prompt air-scattered neutrons by setting a "window" on the direct-neutron time peak.

V. DETAILED SINGLE-SCATTERING FORMULATION

Several approximations found in Section III and IV can be relaxed in order to provide a more general treatment of air scattering. Those features of the problem which will be taken into consideration in the present section are:

a. The angular distribution and variation of energy with emission angle for neutrons from the source.

b. Attenuation of both primary and air-scattered neutrons by intervening air.

c. Energy loss by neutrons in elastic and inelastic scattering from nitrogen and oxygen.

d. Angular distribution effects in elastic scattering from nitrogen and oxygen.

e. Finite thickness of the uranium deposit in the fission chamber.

f. Variations in the isotopic content of the fission deposit and energy dependence of the fission cross section.

The quantity F_2 is defined as:

F_2 = relative number of fissions produced in the fission detector by air-scattered and primary neutrons.

Monte-Carlo methods similar to those used for calculation of F_1 in Section IV have been applied in calculation of F_2. The parameters r_A, ϕ_A, Z_A and r_F were selected at random and computation was limited to the region of space defined by $R_{A,MAX}$ and $Z_{A,MAX}$ as described in Section IV. Thus

$$F_2 \approx 2\pi\, R_{A,MAX} Z_{A,MAX} \frac{\left[\left(\sum_{j=1}^{N_{HIST}} \mathcal{R}_j\right) / N_{HIST}\right]}{\left[\left(\sum_{j=1}^{M_{HIST}} \mathcal{R}_j\right) / M_{HIST}\right]} \tag{28}$$

where for each j,

$$\mathcal{R} = f_{SO} \cos\theta_{SO} \left(\frac{r_f}{d_0^2}\right) \exp\left(-d_0 \Sigma_{T,AIR,O}\right) X \tag{29}$$

$$X \left(\frac{\Sigma_{F,U,0}}{\Sigma_{T,U,0}}\right) \left[1 - \exp\left(-\tau\Sigma_{T,U,0}/\cos\theta_{S0}\right)\right]$$

and

$$\mathcal{S} = f_{S1} \cos\theta_I \left(\frac{r_A r_F}{d_1^2 d_2^2}\right) \exp\left(-d_1\Sigma_{T,AIR,1}\right) X$$

$$X \left\{ \sum_{k=1}^{3} \left(\frac{\delta\Sigma}{\delta\Omega} AIR,1k\right) \exp\left(-d_2\Sigma_{T,AIR,2}\right) X \right.$$

$$\left. X \left(\frac{\Sigma_{F,U,2k}}{\Sigma_{T,U,2k}}\right) \left[1 - \exp\left(-\tau\Sigma_{T,U,2k}/\cos\theta_I\right)\right] \right\} \tag{30}$$

with

f_{S0} = neutron source strength as a function of angle

θ_{S0} = neutron emission angle.

$\left(\frac{\delta\Sigma}{\delta\Omega} AIR,1k\right)$ = normalized macroscopic differential cross section for the k-th scattering process for air.

τ = uranium deposit thickness.

The subscript "T" designates a total cross section. The subscript "F" designates a fission cross section. The subscripts "0", "1" and "2" designate the neutron paths with respective lengths d_0, d_1 and d_2 as shown in Fig. 3. The subscript "U" designates a process involving the uranium deposit. Finally the subscript "k" designates a particular neutron scattering process in air (k = 1: nitrogen elastic scattering, k = 2: nitrogen inelastic scattering, and k = 3: oxygen elastic scattering). All cross sections designated by a "Σ" are macroscopic.

A digital computer was utilized for calculations of F_2. A listing of the FORTRAN IV code AIRSC2 employed in the calculations

appears in Appendix II. Changes in neutron energy following a scattering process (e.g. Ref. 6) can be calculated with AIRSC2. Thus it was possible to determine a distribution of fission events vs. incident neutron energy. This distribution function is quite useful since it enables one to deduce an average energy for scattered neutrons incident on the uranium deposit.

Calculations were made for U-235 enriched deposits and also for deposits which were enriched in U-238. See Table VI for the deposit compositions used in most of the calculations. The deposits were assumed to be uniformly thick. Fission cross sections required for this work were obtained from the ENDF/B-III set [7], from compilations by W. G. Davey [8,9] and from measurements by Meadows [10] (see Table VII for values of these cross sections).

The first set of calculations was carried out with the intent of comparing predictions from the detailed single-scattering formulation with those from Sections III and IV for several neutron energies and a fixed geometry. The parameters used for these calculations are indicated in Table VIII. Unless otherwise stated, the parameters for all other sets of calculations discussed in this section are those from Table VIII. Integrations were carried out over a finite air volume ($R_{A,MAX} = Z_{A,MAX} = 30$ cm). Resultant F_2 values were corrected for excluded space by means of data from Fig. 5. Fig. 10 is a plot of F_0 and F_2 for both a U-235 enriched and a U-238 enriched deposit (see Table VI) vs. source neutron energy. The agreement of F_2 and F_0 [computed from Eqs. (10) and (11)] is reasonably good at most energies for the U-235 monitor. The agreement is poor over the energy range 0.85 - 2 MeV for the U-238 monitor. The explanation for this result is that the U-238 fission cross section increases sharply at $E_n \gtrsim 1$ MeV and those neutrons which are scattered by air generally lose sufficient energy so that they contribute far fewer fissions per neutron than the primary neutrons. At higher energies, the neutron energies after scattering remain above this threshold region. Figs. 11 and 12 are plots of the number of fissions vs. the energy of incidence of scattered neutrons at a U-235 enriched and U-238 enriched

deposit respectively. The effect of air scattering on the neutron energy spectra is evident. Spectral plots for 5 MeV primary energy show the effect of inelastic scattering from nitrogen. The inelastically scattered neutrons have very little effect on a U-238 deposit below $\sim$ 5 MeV because the U-238 fission cross section is small for the low-energy inelastically scattered neutrons.

Next, the influence of uranium deposit thickness on the calculation of F_2 was investigated. Calculations were made only for U-235 enriched deposits. Deposits with thicknesses ranging from 0.001 to 1000 times that for the deposit described in Table VI were considered. Otherwise, the parameters employed were those indicated in Table VIII. A primary energy of 1 MeV was assumed for this set of calculation. The results appear in Table IX. Clearly, F_2 is insensitive to the deposit thickness for all realistic deposits.

The detailed formulation is capable of taking the neutron source distribution into consideration, so this aspect was investigated next. In order to make a systematic investigation, hypothetical neutron source distributions of the form

$$S(\theta_{LAB}) = 1 + w_1 P_1 (\cos \theta_{LAB}) \tag{31}$$

were assumed and w_1 was varied from $w_1 = -1$ (strong backward peaking) through $w_1 = 0$ (isotropic) to $w_1 = 1$ (strong forward peaking). The calculations were made assuming a monoenergetic neutron source of 1 MeV. Otherwise, the parameters of the calculation were as indicated in Table VIII. Resulting values of F_2 are plotted in Fig. 13. The conclusion from this analysis is that the ratio of fissions from air-scattered neutrons and primary neutrons is only moderately sensitive to the neutron source distribution provided that the distribution is more or less forward peaked ($0 < w_1 \leq 1$). However, the relative contribution from air-scattered neutrons increases sharply if the source distribution is more or less backward peaked ($-1 \leq w_1 < 0$). In the latter case, the approximate treatments of Sections III and IV do not give reasonable values for the air scattering correction. In practice, most neutron source reactions tend to emit neutrons pre-

dominantly at forward laboratory angles.

The preceding calculations assumed monoenergetic neutrons from the source. In practice, neutron energy varies with emission angle because of the kinematics of source reactions involving finite nuclei. In order to investigate the effect of neutron source kinematic broadening, calculations were performed assuming hypothetical two-body neutron producing reactions with Q = 0 initiated by a projectile with mass equal to a neutron (A_1 = 1.009 amu). Target nuclei with masses (in amu) A_2 = 2,5,10,20,50, 100 and infinity were considered. The neutron source distributions were assumed to be isotropic. Other parameters of the calculation were as indicated in Table VIII. Calculations were made with primary projectile energies E_1 = 1 MeV and 3 MeV for both U-235 and U-238 enriched deposits. The results of these calculations appear in Table X. The conclusion to be drawn from these results is that F_2 is only moderately sensitive to target mass A_2 for a U-235 enriched deposit. The sensitivity is somewhat greater for a U-238 enriched monitor, presumably because of the more pronounced energy dependency of the fission cross section for U-238.

The influence of the nitrogen and oxygen elastic scattering angular distributions cannot be very large because the agreement of F_0 from Section III and F_2 calculated for similar geometry and neutron source characteristics is fairly good except for a U-238 enriched deposit when E_n = 0.85 - 2 MeV. In order to check this point further, calculations were made for several primary energies with the nitrogen scattering assumed to be isotropic and then with the oxygen scattering assumed isotropic. All other parameters were as indicated in Table VIII. The results of this analysis appear in Table XI. As expected, the substitution of isotropy for either nitrogen or oxygen elastic scattering has a relatively moderate effect on F_2.

A final application of the detailed single scattering formulation was to calculate F_2 for a realistic neutron source reaction. Angular distributions for the $^7Li(p,n)^7Be$ reaction, which produces

two distinct groups having Q-values of -1.644 and -2.079 MeV respectively, have been measured for several proton energies by S. A. Elbakr et al. [11]. Coefficients for these distributions, expressed in the laboratory system, are given in Table XII for reference. The results of calculations for a U-235 deposit appear in Fig. 14. Except for the neutron source specifications, the parameters indicated in Table VIII were used in these calculations. Fig. 15 shows the results from a similar set of calculations for a U-238 enriched deposit. Generally, the values of F_2 are smaller for the $^7Li(p,n)^7Be$ neutron groups than for an isotropic, mono-energetic source. An exception is the set of F_2 values for a U-235 deposit and the Q = 2.079 MeV group from the $^7Li(p,n)^7Be$ reaction.

VI. CONCLUSIONS

The number of air scattered neutrons incident upon a fission chamber is small relative to the direct flux for most experimental configurations. The relative importance of air-scattered neutrons is dominated by the distance d from the source to the fission deposit and by the mean free path λ_E for elastic scattering. These two parameters enter as the ratio (d/λ_E). The effect of air scattering generally decreases with increased neutron energy; however, there is a sharp increase in the vicinity of the 0.44 MeV oxygen resonance. Since most of the air scattering occurs near to the source, it is not possible to discriminate against the air-scattered neutrons by means of time of flight. Kinematic broadening of source neutron energies and the shapes of nitrogen and oxygen elastic scattering angular distributions have only a moderate effect on air scattering. The relative importance of air scattering is very sensitive to the angular distribution of the source neutrons and is observed to increase sharply if the source peaks toward back angles. The effect of air scattering on a U-238 enriched deposit is smaller than that for a U-235 deposit for neutrons in the vicinity of 0.82 - 2 MeV where the U-238 fission cross section increases rapidly with energy. The ex-

planation for this effect is that air scattering degrades the neutron energies into a region where the U-238 fission cross section is small. This phenomenon could introduce a noticeable error in measurement of the ratio of the U-238 to U-235 fission cross sections. For example, consider a hypothetical measurement made with a double fission chamber containing two uranium deposits (one enriched in U-235 and the second enriched in U-238) on adjacent backing plates 10 cm from an isotropic fast-neutron source. From Fig. 10 we can deduce that the air-scattering correction is $\sim$ 0.3% for U-235 and $\sim$ 0.06% for U-238 at E_n = 1.5 MeV. Consequently, there is a net correction of $\sim$ 0.24% in the cross section ratio. This is not a negligible correction since experimenters are currently striving for accuracies of $\lesssim$ 1% in fission cross section ratio measurements.

ACKNOWLEDGEMENTS

The author is indebted to J. W. Meadows, P. T. Guenther and A. B. Smith for valuable suggestions which they made during the course of this work.

REFERENCES

1. Handbook of Chemistry and Physics, 41st Edition, ed. C. D. Hodgman, Chemical Rubber Publishing Company, Cleveland, Ohio, U.S.A. (1959).
2. C. A. Rohrman, "Chart of the Nuclides", compiled at Battelle-Northwest, Richland, Washington 99352, U.S.A., for the U.S. Atomic Energy Commission (1969).
3. J. H. Ray, G. Grochowski and E. S. Troubetzkoy, "Neutron Cross Sections of Nitrogen, Oxygen, Aluminum, Silicon, Iron, Deuterium and Beryllium", Report No. UNC-5139, United Nuclear Corporation, Elmsford, New York 10523 (1965).
4. R. W. Lamphere, "Fission Detectors", in Fast Neutron Physics I eds. J. B. Marion and J. L. Fowler, Interscience, New York, 449 (1960).
5. A. Langsdorf, Jr., "Neutron Collimation and Shielding for Experimental Purposes", in Fast Neutron Physics I, eds. J. B. Marion and J. L. Fowler, Interscience, New York, 721 (1960).
6. A. S. Langsdorf, J. E. Monahan and W. A. Reardon, "A Tabulation of Neutron Energies from Monoenergetic Protons on Lithium", Report No. ANL-5219, Argonne National Laboratory, Argonne, Illinois 60439 (1954).
7. National Neutron Cross Section Center, Brookhaven National Laboratory, Upton, New York 11973, U.S.A.
8. W. G. Davey, "Selected Fission Cross Sections for ^{232}U, ^{233}U, ^{234}U, ^{235}U, ^{236}U, ^{237}Np, ^{238}U, ^{239}Pu, ^{241}Pu and ^{242}Pu", Nuclear Science and Engineering 32, 35 (1969).
9. W. G. Davey, "An Analysis of the Fission Cross Sections of ^{232}Th, ^{233}U, ^{234}U, ^{235}U, ^{236}U, ^{237}Np, ^{238}U, ^{239}Pu, ^{241}Pu and ^{242}Pu from 1 keV to 10 MeV", Nuclear Science and Engineering 26, 149 (1966).
10. J. W. Meadows, "The Ratio of the Uranium-238 to Uranium-235 Fission Cross Sections from 1 to 5 MeV", Nuclear Science and Engineering 49, 310 (1972).
11. S. A. Elbakr, I. J. Van Heerden, W. J. McDonald and G. C. Neilson, "Measurements of Neutron Angular Distributions from the $^{7}Li(p,n)^{7}Be$ Reaction", Nuclear Instruments and Methods 105, 519 (1972).

TABLE I

Selected Cross Section Values for N-14[a]

Total Cross Sections

E_n (MeV)	$\sigma_{T,N}$ (barns)	E_n (MeV)	$\sigma_{T,N}$ (barns)	E_n (MeV)	$\sigma_{T,N}$ (barns)
0.0[b]	10.5	1.096	2.48	2.438	1.51
0.01	7.8	1.152	1.73	2.833	1.48
0.403	3.29	1.211	1.61	2.978	1.66
0.424	5.01	1.273	1.86	3.131	1.67
0.455	3.35	1.338	2.83	3.292	1.73
0.468	2.59	1.479	2.07	3.638	1.75
0.601	1.8	1.555	2.37	3.824	1.69
0.632	1.91	1.635	2.4	4.226	1.71
0.665	2.38	1.718	2.05	4.443	1.78
0.7	2.29	1.806	2.46	4.671	1.86
0.734	2.06	1.899	1.85	4.91	1.37
0.943	1.26	2.099	1.58	5.162	1.63
0.991	1.55	2.206	1.66		
1.042	2.21	2.32	1.56		

TABLE I (Contd.)

Elastic Scattering Cross Sections

E_n (MeV)	$\sigma_{E,N}$ (barns)	E_n (MeV)	$\sigma_{E,N}$ (barns)	E_n (MeV)	$\sigma_{E,N}$ (barns)
0.0[b]	10.5	1.152	1.72	3.131	1.36
0.01	7.8	1.211	1.596	3.292	1.36
0.403	3.29	1.273	1.84	3.46	1.34
0.424	5.01	1.338	2.73	3.638	1.37
0.455	3.35	1.479	1.95	3.824	1.33
0.468	2.59	1.555	2.32	4.02	1.24
0.601	1.8	1.635	2.35	4.226	1.23
0.632	1.76	1.718	2.0	4.443	1.35
0.665	2.21	1.806	2.3	4.671	1.46
0.699	2.23	1.899	1.77	4.91	1.05
0.734	2.03	2.695	1.25	5.16	1.32
0.943	1.25	2.833	1.24		
1.096	2.48	2.978	1.39		

Inelastic Scattering Cross Sections (Q=-3.945 MeV)

E_n (MeV)	$\sigma_{I,N}$ (barns)	E_n (MeV)	$\sigma_{I,N}$ (barns)	E_n (MeV)	$\sigma_{I,N}$ (barns)
0.0[b]	0.0	4.226	6.763×10^{-3}	5.0	1.0×10^{-2}
3.945	0.0	4.443	7.73×10^{-3}		
4.02	1.751×10^{-3}	4.671	8.583×10^{-3}		

TABLE I(Contd.)

a. Values taken from Ref. 3.

b. A "zero-energy" cross section value is included in the tables to provide a lower limit for interpolation.

TABLE II

Selected Cross Section Values for O-16[a]

Total Cross Sections

E_n (MeV)	$\sigma_{T,0}$ (barns)	E_n (MeV)	$\sigma_{T,0}$ (barns)	E_n (MeV)	$\sigma_{T,0}$ (barns)
0.0[b]	3.7	1.152	3.03	2.563	1.23
0.284	3.71	1.211	3.01	2.695	1.22
0.383	4.26	1.273	4.55	2.833	1.28
0.403	6.04	1.338	3.8	3.131	1.8
0.424	11.2	1.479	2.28	3.292	2.86
0.445	14.5	1.555	2.28	3.46	3.02
0.468	9.5	1.635	3.47	4.02	1.7
0.492	5.71	1.718	3.02	4.226	1.82
0.518	4.28	1.899	2.72	4.443	1.88
0.544	3.64	2.099	1.4	4.671	1.11
0.853	3.03	2.32	0.779	4.91	1.13
0.991	7.47	2.438	0.919	5.162	1.6

TABLE II (Contd.)

Elastic Scattering Cross Sections

E_n (MeV)	$\sigma_{E,0}$ (barns)	E_n (MeV)	$\sigma_{E,0}$ (barns)	E_n (MeV)	$\sigma_{E,0}$ (barns)
0.0[b]	3.7	1.211	3.01	2.695	1.22
0.383	4.26	1.273	4.55	2.833	1.28
0.403	6.04	1.338	3.8	3.131	1.8
0.424	11.2	1.479	2.28	3.292	2.86
0.445	14.5	1.555	2.28	3.46	3.02
0.468	9.5	1.635	3.47	3.638	2.98
0.492	5.71	1.718	3.02	3.82	2.89
0.518	4.28	1.899	2.72	4.02	1.63
0.544	3.64	2.099	1.4	4.443	1.84
0.853	3.03	2.32	0.779	4.671	1.06
0.991	7.47	2.438	0.919	4.91	1.03
1.152	3.03	2.563	1.23	5.162	1.54

a. Values taken from Ref. 3.

b. A "zero-energy" cross section value is included in the table to provide a lower limit for interpolation.

TABLE III

Legendre Coefficients for Nitrogen Laboratory Elastic-Scattering Angular Distributions[a]

W_1

E_n (MeV)	W_1	E_n (MeV)	W_1	E_n (MeV)	W_1
0.0[b]	0.14	1.4	0.58	3.0	0.2
1.0	0.305	1.48	0.48	3.4	0.2
1.02	0.19	1.62	0.75	4.25	0.8
1.15	0.66	1.8	0.25	4.95	0.5
1.3	0.3	2.25	0.74	5.4	0.51

W_2

E_n (MeV)	W_2	E_n (MeV)	W_2	E_n (MeV)	W_2
0.0[b]	0.0	1.45	0.14	3.12	1.56
1.0	0.0	1.8	0.69	3.45	1.78
1.15	0.45	2.1	0.24	3.92	1.91
1.25	0.21	2.45	0.65	4.25	1.83
1.35	0.375	2.8	1.24	5.15	0.96

TABLE III (Contd.)

W_3

E_n (MeV)	W_3	E_n (MeV)	W_3	E_n (MeV)	W_3
0.0[b]	0.0	1.65	0.2	2.7	2.7
1.0	0.0	1.7	0.11	3.3	0.35
1.2	0.21	2.1	0.12	4.25	0.57
1.35	0.13	2.35	0.35	5.15	0.65

W_4

E_n (MeV)	W_4	E_n (MeV)	W_4	E_n (MeV)	W_4
0.0[b]	0.0	3.46	0.641	4.671	0.743
2.9	0.0	3.824	0.549	4.91	0.854
2.978	0.074	4.02	0.458	5.162	0.731
3.131	0.32	4.23	0.453		
3.292	0.499	4.443	0.546		

TABLE III (Contd.)

W_5

E_n (MeV)	W_5	E_n (MeV)	W_5	E_n (MeV)	W_5
0.0[b]	0.0	4.443	0.136	4.91	0.498
4.4	0.0	4.671	0.303	5.162	0.534

a. Legendre coefficients are derived from data in Ref. 3. Angular distributions may be calculated from Eq. (3), however the coefficients listed above or interpolated values may not yield proper normalization. The computed distributions should be renormalized prior to use in scattering calculations.

b. A "zero-energy" coefficient value is included in the table to provide a lower limit for interpolation.

TABLE IV

Legendre Coefficients for Oxygen Laboratory Elastic-Scattering Angular Distributions[a]

W_1

E_n (MeV)	W_1	E_n (MeV)	W_1	E_n (MeV)	W_1
0.0[b]	0.12	1.33	1.02	3.64	1.16
0.15	0.06	1.5	0.24	3.83	1.0
0.36	-0.59	1.7	0.0	4.05	1.01
0.46	1.32	2.05	0.42	4.25	0.77
0.8	0.3	2.5	0.08	4.45	1.39
1.0	0.22	2.95	0.34	4.85	0.4
1.05	-0.06	3.13	0.73	5.17	0.38
1.2	-0.18	3.3	0.56		

W_2

E_n (MeV)	W_2	E_n (MeV)	W_2	E_n (MeV)	W_2
0.0[b]	0.0	1.02	1.65	3.3	1.58
0.1	0.0	1.5	0.24	4.05	0.82
0.35	-0.26	1.65	0.48	4.45	1.46
0.43	0.81	1.7	0.18	4.67	0.3
0.58	0.08	2.1	0.64	5.15	0.98
0.82	-0.16	2.45	-0.02		
0.9	-0.06	3.0	0.26		

TABLE IV (Contd.)

W_3

E_n (MeV)	W_3	E_n (MeV)	W_3	E_n (MeV)	W_3
0.0[b]	0.02	1.55	0.3	3.62	0.94
0.25	-0.095	1.64	0.62	3.85	0.94
0.4	0.24	1.75	0.3	4.15	0.6
0.65	-0.02	2.0	0.075	4.45	1.46
0.85	-0.04	2.7	0.02	4.7	0.82
0.98	0.38	3.0	0.18	5.15	1.22
1.15	-0.1	3.2	0.86		
1.4	0.48	3.45	0.6		

W_4

E_n (MeV)	W_4	E_n (MeV)	W_4	E_n (MeV)	W_4
0.0	0.0	1.1	-0.02	3.3	0.01
0.2	0.18	1.25	0.26	3.62	0.33
0.32	-0.08	1.4	0.12	4.1	0.04
0.43	0.14	1.52	0.8	4.5	0.56
0.52	-0.07	1.73	0.32	4.7	0.46
0.6	0.064	2.4	0.0	5.15	0.76
0.8	-0.04	2.55	0.065		
0.93	0.16	2.83	-0.04		

TABLE IV (Contd.)

w_5

E_n (MeV)	w_5	E_n (MeV)	w_5	E_n (MeV)	w_5
0.0[b]	0.0	1.05	0.02	3.62	0.18
0.15	-0.04	1.4	-0.05	3.95	-0.06
0.35	0.24	1.63	0.8	4.22	0.04
0.5	-0.02	1.95	0.02	4.7	-0.1
0.8	0.06	2.55	0.04	5.7	0.32
0.95	0.52	3.1	-0.1		

a. Legendre coefficients are derived from data in Ref. 3. Angular distributions may be calculated from Eq. (3), however the coefficients listed above or interpolated values may not yield proper normalization. The computed distributions should be renormalized prior to use in scattering calculations.

b. A "zero-energy" coefficient value is included in the table to provide a lower limit for interpolation.

TABLE V

Mean Free-Path for Neutron Elastic Scattering in Air[a]

E_n (MeV)	λ_E (cm)	E_n (MeV)	λ_E (cm)	E_n (MeV)	λ_E (cm)
0.05	2973	0.55	8097	2.0	11030
0.1	3185	0.6	9052	2.25	13780
0.15	3429	0.7	7984	2.5	14920
0.2	3714	0.8	9490	2.75	15740
0.25	4050	0.85	10330	3.0	13760
0.3	4454	0.9	9495	3.25	12140
0.35	4947	1.0	6854	3.5	11570
0.375	5236	1.1	6876	3.75	11700
0.4	5111	1.2	10260	4.0	14470
0.425	3115	1.3	7445	4.5	13680
0.45	3461	1.4	7712	5.0	16890
0.475	5200	1.5	9338		
0.5	6536	1.75	8568		

a. Values of λ_E computed from Eq. (11).

TABLE VI

Uranium Deposit Compositions Assumed for the Calculations in Section V

U-235 Enriched Deposit

U-234	content	=	0.856%	Total mass 878 micrograms
U-235	content	=	93.249%	
U-236	content	=	0.332%	
U-238	content	=	5.526%	

U-238 Enriched Deposit

U-235	content	=	0.415%	Total mass 2398 micrograms
U-238	content	=	99.585%	

U-234 and U-236 contents are negligible

TABLE VII

Fission Cross Sections Used in the Present Work

U-234(n,f) Cross Sections

E_n (MeV)	$\sigma_{F,234}$ (barns)	E_n (MeV)	$\sigma_{F,234}$ (barns)	E_n (MeV)	$\sigma_{F,234}$ (barns)
0.0	0.0[a]	1.0	1.092[a]	6.0	1.422[a]
0.01	0.01[a]	1.8	1.48[a]	7.0	1.773[a]
0.1	0.024[a]	2.0	1.508[a]	8.0	1.972[a]
0.25	0.06[a]	2.4	1.444[a]	9.0	2.012[a]
0.4	0.262[a]	3.5	1.383[a]	10.2	1.810[a]
0.6	0.683[a]	4.5	1.275[a]	12.5	1.813[a]
0.7	1.085[a]	5.0	1.261[a]	15.0	1.996[a]
0.8	1.26[a]	5.5	1.308[a]		

U-235(n,f) Cross Sections

E_n (MeV)	$\sigma_{F,235}$ (barns)	E_n (MeV)	$\sigma_{F,235}$ (barns)	E_n (MeV)	$\sigma_{F,235}$ (barns)
0.0	580.0[b]	0.8	1.133[a]	6.1	1.098[a]
1.0×10^{-6}	65.0[b]	0.85	1.15[a]	6.3	1.164[a]
0.001	8.05[b]	0.95	1.218[a]	6.8	1.413[a]
0.003	4.99[b]	1.0	1.235[a]	7.2	1.552[a]
0.01	3.21[b]	1.5	1.247[a]	7.6	1.634[a]
0.0175	2.7[b]	2.0	1.315[a]	8.5	1.751[a]
0.03	2.27[b]	2.3	1.309[a]	9.5	1.753[a]
0.055	1.91[b]	2.6	1.281[a]	10.5	1.7[a]
0.1	1.635[a]	3.2	1.177[a]	11.5	1.7[a]
0.16	1.478[a]	3.6	1.146[a]	12.5	1.82[a]
0.24	1.32[a]	4.2	1.089[a]	13.0	2.0[a]
0.35	1.225[a]	4.8	1.056[a]	14.0	2.13[a]
0.4	1.218[a]	5.4	1.046[a]	15.0	2.16[a]
0.54	1.16[a]	5.8	1.068[a]		

TABLE VII (Contd.)

U-236(n,f) Cross Sections

E_n (MeV)	$\sigma_{F,236}$ (barns)	E_n (MeV)	$\sigma_{F,236}$ (barns)	E_n (MeV)	$\sigma_{F,236}$ (barns)
0.0	0.0[a]	2.0	0.828[a]	7.0	1.432[a]
0.7	0.027[a]	2.4	0.882[a]	7.85	1.73[a]
0.9	0.292[a]	2.8	0.872[a]	9.0	1.84[a]
1.2	0.61[a]	5.0	0.868[a]	11.5	1.722[a]
1.4	0.69[a]	5.5	0.822[a]	13.5	1.657[a]
1.6	0.688[a]	6.0	0.903[a]	15.0	1.625[a]

U-238(n,f) Cross Sections

E_n (MeV)	$\sigma_{F,238}$ (barns)	E_n (MeV)	$\sigma_{F,238}$ (barns)	E_n (MeV)	$\sigma_{F,238}$ (barns)
0.0	0.0[a]	1.514	0.3458[c]	4.47	0.5339[c]
0.5	2.34×10^{-4}[a]	1.617	0.4169[c]	5.08	0.5324[c]
0.61	1.24×10^{-3}[a]	1.72	0.4472[c]	5.33	0.5403[c]
0.75	1.98×10^{-3}[a]	1.821	0.5122[c]	6.0	0.618[a]
0.85	5.87×10^{-3}[a]	1.914	0.5397[c]	7.0	0.936[a]
0.898	0.0123[c]	2.0	0.5371[c]	7.5	0.978[a]
1.005	0.0163[c]	2.51	0.5573[c]	8.5	1.0[a]
1.108	0.0273[c]	3.08	0.525[c]	10.0	0.974[a]
1.205	0.0374[c]	3.28	0.5242[c]	12.0	0.995[a]
1.306	0.0651[c]	3.58	0.5352[c]	13.5	1.098[a]
1.401	0.1939[c]	4.08	0.5336[c]	15.0	1.25[a]

a. Values obtained from ENDF/B-III evaluation [7].

b. Values obtained from Davey compilation [20,21].

c. Values calculated using ENDF/B-III values of $\sigma_{F,235}$ [6] and Meadows U-238 to U-235 fission cross section ratios [11].

TABLE VIII

Normal Parameter Set for Air Scattering Calculations with the Detailed Single Scattering Formulation Described in Section V

1. Total, elastic and inelastic scattering cross sections for nitrogen (Table I).
2. Elastic scattering angular distribution coefficients for nitrogen (Table III).
3. Total and elastic scattering cross sections for oxygen (Table II).
4. Elastic scattering angular distribution coefficients for oxygen (Table IV).
5. Fission cross sections for U-234, U-235, U-236 and U-238. (Table VII).
6. Uranium deposit masses and compositions. (Table VI).
7. Isotropic, monoenergetic neutron point source.
8. Geometric parameters (see Fig. 3):

$$d = 5 \text{ cm}$$
$$R_{DISK} = 1.27 \text{ cm}$$
$$R_{A,MAX} = Z_{A,MAX} = 30 \text{ cm}$$

TABLE IX

Variation of F_2 with Thickness of a U-235 Enriched Deposit[a]

Thickness Multiple	Deposit Weight (gm)	F_2/F_2 (Standard)	
0.001	8.784×10^{-7}	0.965	
0.01	8.784×10^{-6}	1.079	
0.1	8.784×10^{-5}	0.995	Realistic deposit thickness range
0.5	4.392×10^{-4}	1.057	
1[b]	8.784×10^{-4}	1 Standard Deposit	
2	1.757×10^{-3}	1.027	
5	4.392×10^{-3}	1.014	
10	8.784×10^{-3}	0.973	
100	8.784×10^{-2}	1.083	
1000	8.784×10^{-1}	0.987	

a. Values of F_2 were calculated via the techniques of Section V and using the parameters indicated in Table VIII except for the deposit thickness which was variable.

b. The standard deposit is the 878.4 microgram U-235 enriched deposit described in Table VI.

TABLE X

The Effect of Neutron Source Kinematic Broadening on F_2[a]

U-235 Enriched Deposit

A_2 (amu)	F_2 E_1 = 1 MeV	E_1 = 3 MeV
2	$.1980 \times 10^{-2}$	$.1003 \times 10^{-2}$
5	$.1298 \times 10^{-2}$	$.8325 \times 10^{-3}$
10	$.1348 \times 10^{-2}$	$.7209 \times 10^{-3}$
20	$.1267 \times 10^{-2}$	$.7046 \times 10^{-3}$
50	$.1406 \times 10^{-2}$	$.9163 \times 10^{-3}$
100	$.1714 \times 10^{-2}$	$.7979 \times 10^{-3}$
Infinite	$.1644 \times 10^{-2}$	$.9055 \times 10^{-3}$

U-238 Enriched Deposit

A_2	F_2 E_1 = 1 MeV	E_1 = 3 MeV
2	$.5975 \times 10^{-3}$	$.5553 \times 10^{-3}$
5	$.6581 \times 10^{-3}$	$.7066 \times 10^{-3}$
10	$.6199 \times 10^{-3}$	$.8517 \times 10^{-3}$
20	$.8130 \times 10^{-3}$	$.8260 \times 10^{-3}$
50	$.7485 \times 10^{-3}$	$.8378 \times 10^{-3}$
100	$.8714 \times 10^{-3}$	$.8121 \times 10^{-3}$
Infinite	$.9975 \times 10^{-3}$	$.8649 \times 10^{-3}$

a. Values of F_2 were calculated via the techniques of Section V. Hypothetical two-body neutron producing reactions with Q = 0 which are initiated by a projectile with mass equal to a neutron (A_1 = 1.009 amu) were assumed. Various target nuclei with masses (in amu) A_2 = 2, 5, 10, 20, 50, 100 and infinity were considered. The neutron emission was taken to be isotropic and other parameters required for the calculations described in Section V were taken from Table VIII.

TABLE XI

Sensitivity of F_2 to the Assumed Elastic Scattering Angular Distributions for Nitrogen and Oxygen[a]

U-235 Enriched Deposit

Normal Oxygen Distribution

E_1 (MeV)	F_2 Normal Nitrogen Distr.	F_2 Isotropic Nitrogen Distr.
1.0	$.1644 \times 10^{-2}$	$.1664 \times 10^{-2}$
1.8	$.1390 \times 10^{-2}$	$.1500 \times 10^{-2}$
2.5	$.6691 \times 10^{-3}$	$.7951 \times 10^{-3}$
3.0	$.9055 \times 10^{-3}$	$.9284 \times 10^{-3}$
3.5	$.1323 \times 10^{-2}$	$.1072 \times 10^{-2}$
5.0	$.8964 \times 10^{-3}$	$.8587 \times 10^{-3}$

Normal Nitrogen Distribution

E_1 (MeV)	F_2 Normal Nitrogen Distr.	F_2 Isotropic Oxygen Distr.
0.45	$.2880 \times 10^{-2}$	$.3933 \times 10^{-2}$
1.0	$.1644 \times 10^{-2}$	$.1607 \times 10^{-2}$
1.8	$.1390 \times 10^{-2}$	$.1510 \times 10^{-2}$
3.5	$.1323 \times 10^{-2}$	$.1208 \times 10^{-2}$
4.5	$.9422 \times 10^{-3}$	$.1463 \times 10^{-2}$

TABLE XI (Contd.)

U-238 Enriched Deposit

Normal Oxygen Distribution

E_1(MeV)	F_2 Normal Nitrogen Distr.	F_2 Isotropic Nitrogen Distr.
1.0	$.9975 \times 10^{-3}$	$.1008 \times 10^{-2}$
1.8	$.9673 \times 10^{-3}$	$.8453 \times 10^{-3}$
2.5	$.6568 \times 10^{-3}$	$.6878 \times 10^{-3}$
3.0	$.8649 \times 10^{-3}$	$.1129 \times 10^{-2}$
3.5	$.1312 \times 10^{-2}$	$.1016 \times 10^{-2}$
5.0	$.7637 \times 10^{-3}$	$.7266 \times 10^{-3}$

Normal Nitrogen Distribution

E_1(MeV)	F_2 Normal Nitrogen Distr.	F_2 Isotropic Nitrogen Distr.
0.45	$.2814 \times 10^{-2}$	$.3364 \times 10^{-2}$
1.0	$.9975 \times 10^{-3}$	$.8696 \times 10^{-3}$
1.8	$.9673 \times 10^{-3}$	$.9059 \times 10^{-3}$
3.5	$.1312 \times 10^{-2}$	$.1272 \times 10^{-2}$
4.5	$.8446 \times 10^{-3}$	$.8709 \times 10^{-3}$

a. Values of F_2 were calculated via the techniques of Section V. The parameters indicated in Table VIII were employed except for the substitution of isotropic elastic scattering angular distributions for nitrogen and oxygen where indicated.

TABLE XII

Coefficients for the Neutron Source Distributions Corresponding to the $^{7}Li(p,n)^{7}Be$ Reaction[a]

First-Group Neutrons (Q = -1.644 MeV)

Proton Energy (MeV)	w_1	w_2	w_3	w_4
2.8	1.19	0.5687	0.1619	0
3.0	1.113	0.4518	0.1075	0
3.2	1.054	0.4437	0.1121	0
3.4	0.9617	0.4044	0.1044	0
3.6	0.8843	0.3655	0.4093	-0.1598×10^{-1}
3.8	0.7795	0.3440	0.7762×10^{-2}	-0.3394×10^{-1}
4.0	0.6877	0.3714	0.1662×10^{-2}	-0.4365×10^{-1}
4.2	0.6097	0.4622	-0.6456×10^{-1}	-0.9487×10^{-1}
4.4	0.5802	0.5519	-0.3219×10^{-1}	-0.8957×10^{-1}
4.6	0.5612	0.6674	0.4624×10^{-1}	-0.6359×10^{-1}
4.8	0.5207	0.6743	0.1318	-0.1948×10^{-1}
5.0	0.4674	0.7297	0.3098	0.6363×10^{-1}

TABLE XII (Contd.)

Second Group Neutrons (Q = -2.079 MeV)

Proton Energy (MeV)	w_1	w_2	w_3	w_4
3.2	0.38	-0.1695	-0.1773	-0.7445×10^{-1}
3.4	0.2859	-0.1582	-0.1427	-0.5812×10^{-1}
3.6	0.1832	-0.443×10^{-1}	-0.4813×10^{-3}	-0.495×10^{-2}
3.8	0.114	0.517×10^{-1}	0.7592×10^{-2}	0.1545×10^{-1}
4.0	-0.3831	0.2217	-0.6469×10^{-1}	0.755×10^{-3}
4.2	-0.4815×10^{-3}	0.223	-0.2205×10^{-2}	-0.5722×10^{-1}
4.4	-0.3763×10^{-1}	0.2364	-0.6162×10^{-2}	-0.6×10^{-1}
4.6	-0.9986×10^{-1}	0.2952	0.2167×10^{-1}	-0.5371×10^{-1}
4.8	-0.7796×10^{-1}	0.3609	-0.6173×10^{-1}	-0.1084
5.0	-0.7609×10^{-1}	0.4322	-0.8369×10^{-1}	-0.1287

a. Laboratory angular distributions for the $^7Li(p,n)^7Be$ reaction were obtained by transformation of the center-of-momentum distributions given by Elbakr et al. [11]. These distributions were fitted with the Legendre expansion

$$S(\Theta_{LAB}) = 1 + \sum_{k=1}^{n} w_k P_k (\cos \Theta_{LAB}).$$

A fourth-order expansion(n=4) was found to be adequate for this purpose.

FIGURE CAPTIONS

Fig. 1. Laboratory neutron elastic-scattering angular distributions for nitrogen computed from the Legendre coefficients given in Table III. The curves were all plotted using the same ordinate scale. The neutron energies shown are in MeV. The negative cross sections appearing at 2.5 MeV are nonphysical and such values were excluded from the scattering calculations. (ANL Neg. No. 116-1904).

Fig. 2. Laboratory neutron elastic-scattering angular distributions for oxygen computed from the Legendre coefficients given in Table IV. The curves were all plotted using the same ordinate normalization. The neutron energies shown are in MeV. Notice the strong forward scattering near the 0.44 MeV resonance. (ANL Neg. No. 116-1912).

Fig. 3. Schematic diagram of a thin uranium deposit in a fission chamber which is placed near a point source of neutrons. (ANL Neg. No. 116-1909).

Fig. 4. The solid curve is a plot of F_0 computed from Eq. (10) using values of λ_E from Table V for d = 5 cm. The individual points are values of F_1 for d = 5 cm and R_{DISK} = 1.27 cm computed via the Monte-Carlo techniques described in Section IV. (ANL Neg. No. 116-1906).

Fig. 5. Plot of the ratio F_1/F_0 computed from Eqs. (10) and (19) for several values of $R_{A,MAX}$ (= $Z_{A,MAX}$) with E_n = 1 MeV, d = 5 cm and R_{DISK} = 1.27 cm. (ANL Neg. No. 116-1905).

Fig. 6. Plot of the ratio F_1/F_0 computed from Eqs. (10) and (19) for several values of d with E_n = 1 MeV, R_{DISK} = 1.27 cm and $R_{A,MAX}$ = $Z_{A,MAX}$ > 10 d. (ANL Neg. No. 116-1913).

Fig. 7. Plot of the average angle of incidence $\bar{\theta}_I$ for several values of d with E_n = 1 MeV, R_{DISK} = 1.27 cm and $R_{A,MAX} = Z_{A,MAX} > 10$ d. Computations were performed according to procedures described in Section IV. (ANL Neg. No. 116-1908).

Fig. 8. Plots of the neutron angle-of-incidence distributions for several values of d with E_n = 1 MeV, R_{DISK} = 1.27 cm and $R_{A,MAX} = Z_{A,MAX} > 10$ d. Computations were performed according to procedures described in Section IV. The distribution function becomes nearly linear when d/R_{DISK} becomes large and the effects of finite uranium deposit size are negligible. (ANL Neg. No. 116-1911).

Fig. 9. Plots of the neutron arrival-time distributions for several neutron energies with R_{DISK} = 1.27 cm, d = 5 cm and $R_{A,MAX} = Z_{A,MAX} > 10$ d. Computations were performed according to procedures described in Section IV. (ANL Neg. No. 116-1910).

Fig.10. Plot of F_0 and of F_2 for a U-235 enriched deposit and for a U-238 enriched deposit. Calculations were performed according to the methods of Sections III and V using the parameters indicated in Table VIII. (ANL Neg. No. 116-1907).

Fig.11. Plots of the relative number of fissions vs. the energy of neutrons incident upon a U-235 enriched deposit. Notice the appearance of an inelastic contribution in the plot for 5 MeV primary energy. Calculations were performed with the methods of Section V and the parameters indicated in Table VIII. (ANL Neg. No. 116-1915).

Fig.12. Plots of the relative number of fissions vs. the energy of neutrons incident upon a U-238 enriched deposit. Notice the appearance of an inelastic contribution in the plot for 5 MeV primary energy. Calculations were performed with the methods of Section V and the parameters indicated in Table VIII. (ANL Neg. No. 116-1914).

Fig.13. Dependence of F_2 on the shape of the neutron source distribution. The insert figures show the neutron source distribution shapes $S(\Theta_{LAB}) = 1 + w_1 P_1(\cos \Theta_{LAB})$ for $w_1 = -1, 0$ and 1. Calculations were made for a primary energy of 1 MeV and additional parameters of the calculations were as indicated in Table VIII. The calculational procedure is described in Section V. Notice that F_2 is very sensitive to the value of w_1 for $-1 \leq w_1 < 0$ (back angle peaking). (ANL Neg. No. 116-1903).

Fig.14. Plot of F_0 and of F_2 for a U-235 enriched deposit. Calculations were made assuming an isotropic, monoenergetic neutron source as well as the Q = -1.644 MeV and Q = -2.079 MeV groups from the $^7Li(p,n)^7Be$ reaction. Other parameters required for these calculations were obtained from Table VIII and the methods of Sections III and IV were used in the analysis. (ANL Neg. No. 116-1916).

Fig.15. Plot of F_0 and of F_2 for a U-238 enriched deposit. Calculations were made assuming an isotropic, monoenergetic neutron source as well as the Q = -1.644 MeV and Q = -2.079 MeV groups from the $^7Li(p,n)^7Be$ reaction. Other parameters required for these calculations were obtained from Table VIII and the methods of Sections III and IV were used in the analysis. (ANL Neg. No. 116-1917).

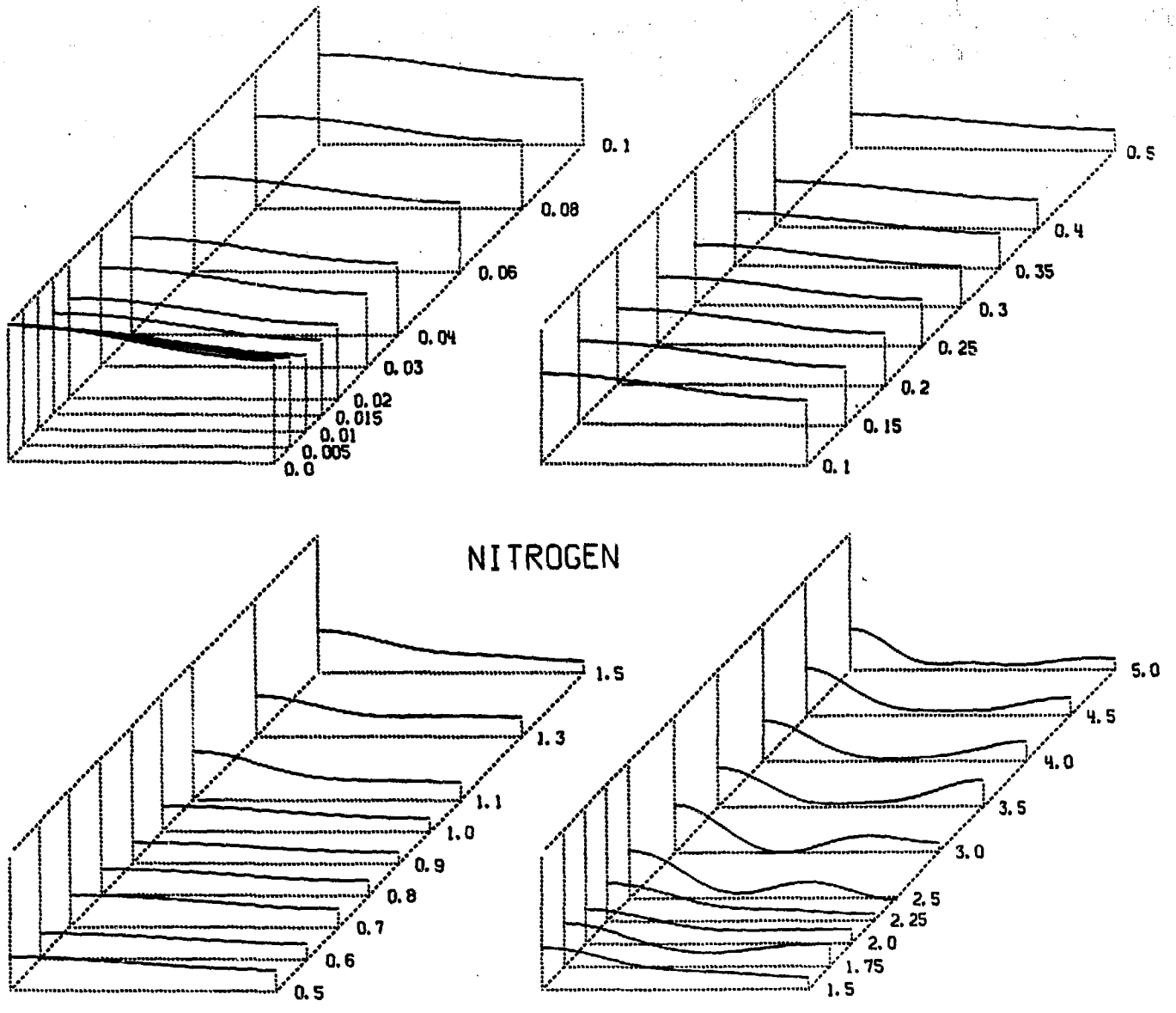
NITROGEN
0.1
0.08
0.06
0.04
0.03
0.02
0.015
0.01
0.005
0.0
0.5
0.4
0.35
0.3
0.25
0.2
0.15
0.1
1.5
1.3
1.1
1.0
0.9
0.8
0.7
0.6
0.5
5.0
4.5
4.0
3.5
3.0
2.5
2.25
2.0
1.75
1.5

Fig. 1

Fig. 2

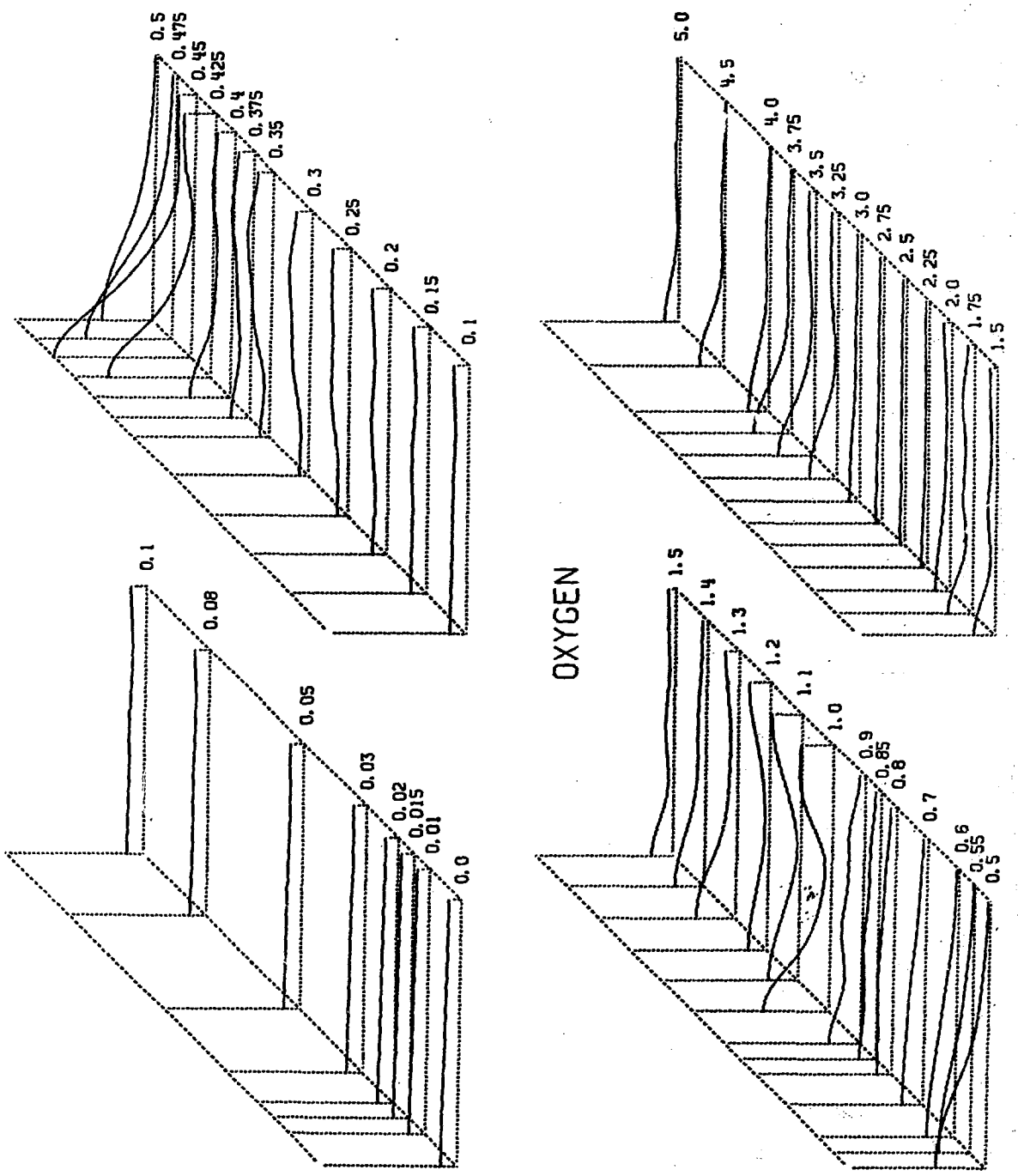
0.5
0.475
0.45
0.425
0.4
0.375
0.35
0.3
0.25
0.2
0.15
0.1
0.1
0.08
0.05
0.03
0.02
0.015
0.01
0.0
OXYGEN
5.0
4.5
4.0
3.75
3.5
3.25
3.0
2.75
2.5
2.25
2.0
1.75
1.5
1.5
1.4
1.3
1.2
1.1
1.0
0.9
0.85
0.8
0.7
0.6
0.55
0.5

Fig. 3

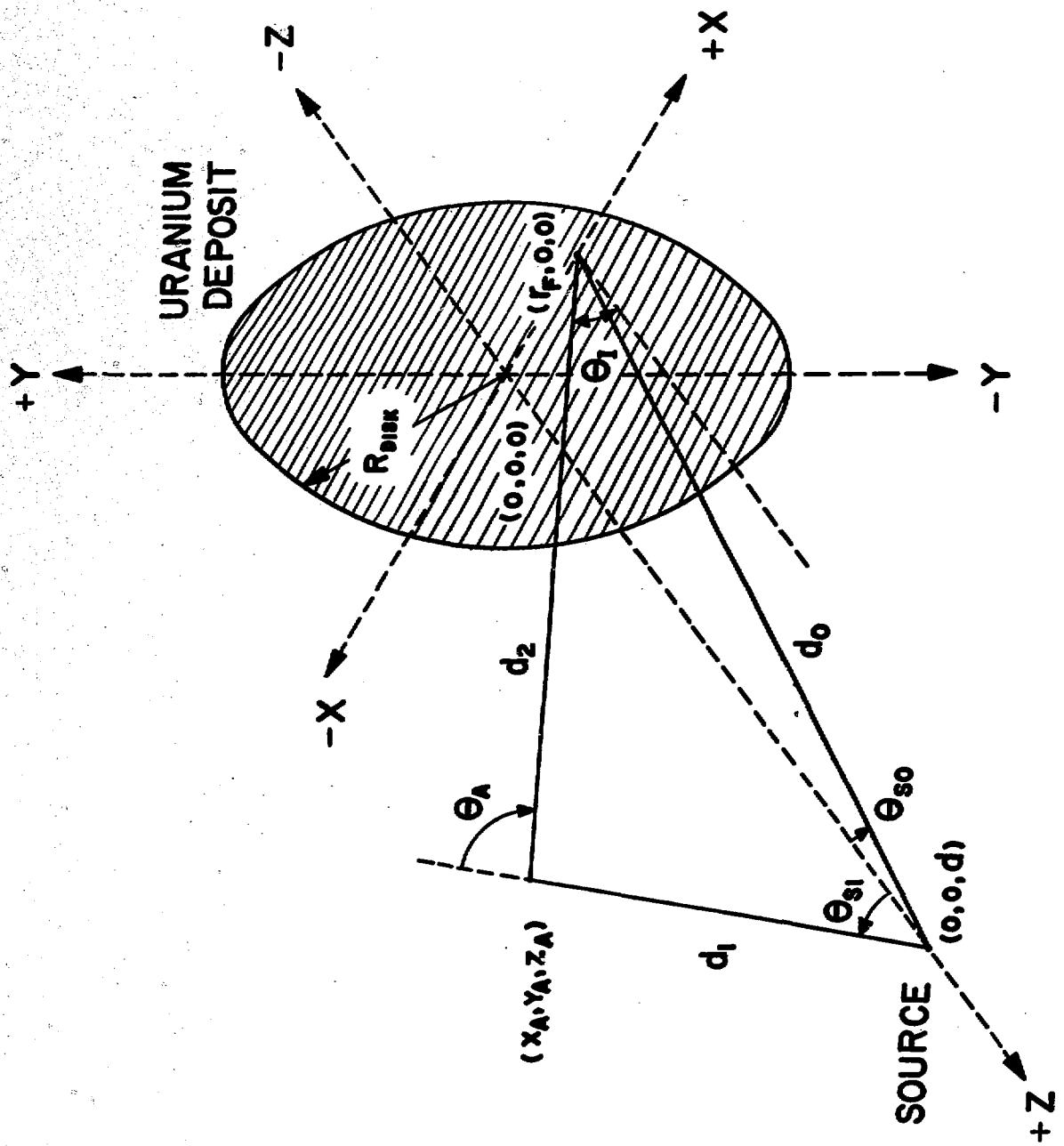
URANIUM
DEPOSIT
+Y
-Y
-Z
+X
-X
+Z
R_{DISK}
(0,0,0)
$(r_F,0,0)$
θ_1
d_2
d_0
θ_A
θ_{SO}
θ_{S1}
d_1
(X_A,Y_A,Z_A)
(0,0,d)
SOURCE

Fig. 4

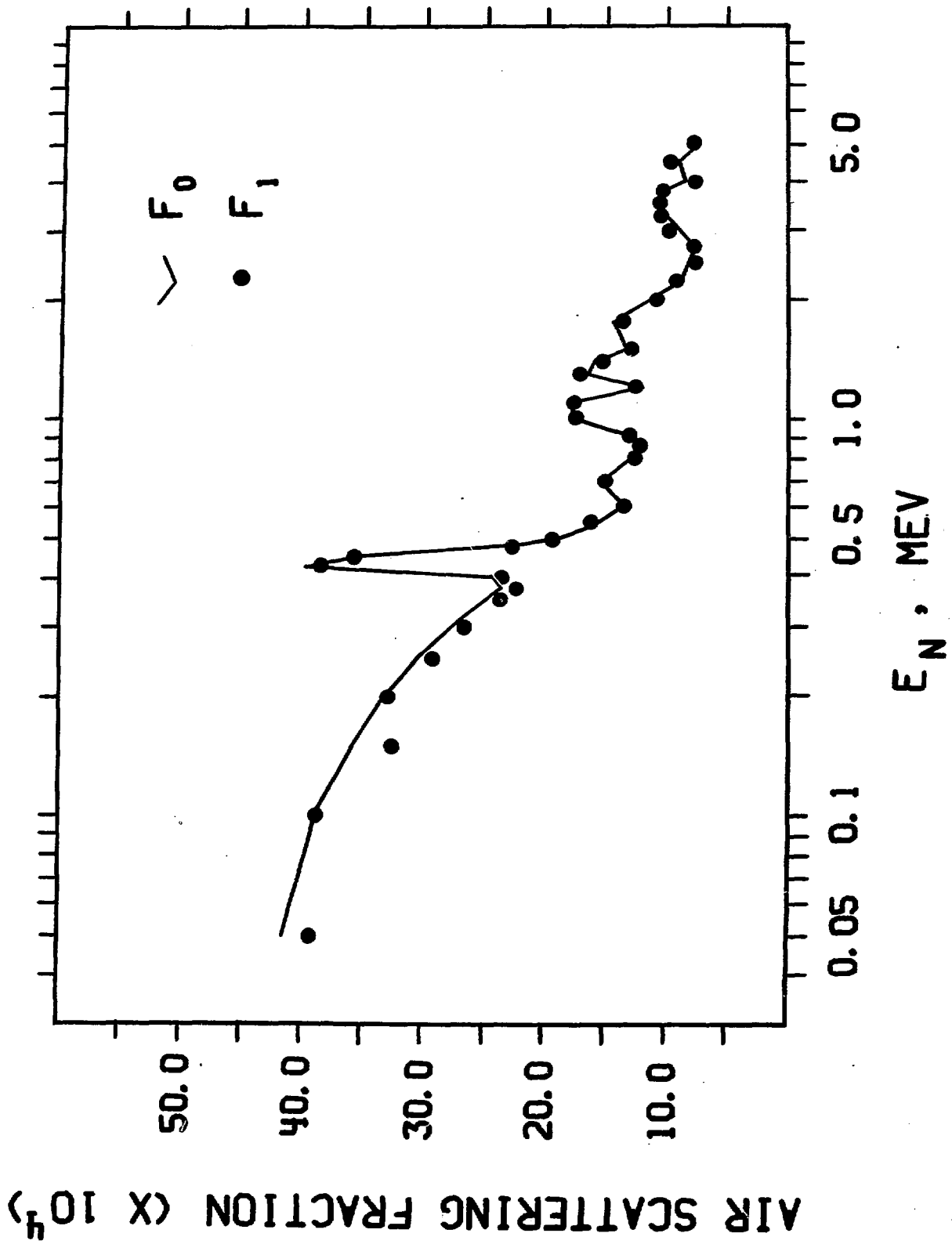
AIR SCATTERING FRACTION (X 10⁴)
50.0
40.0
30.0
20.0
10.0
0.05
0.1
0.5
1.0
5.0
E_N , MEV
F0
F1

Fig. 5

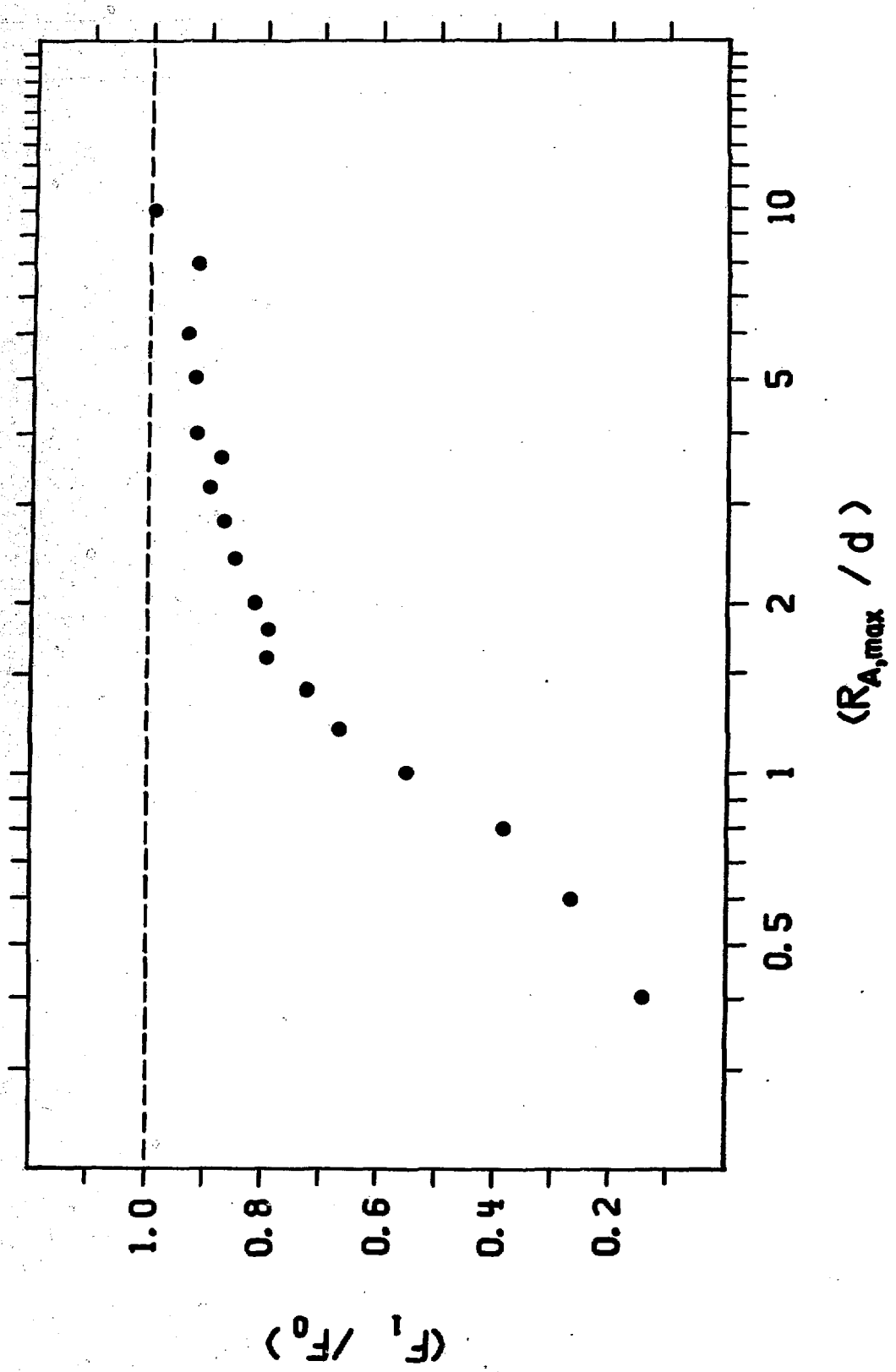

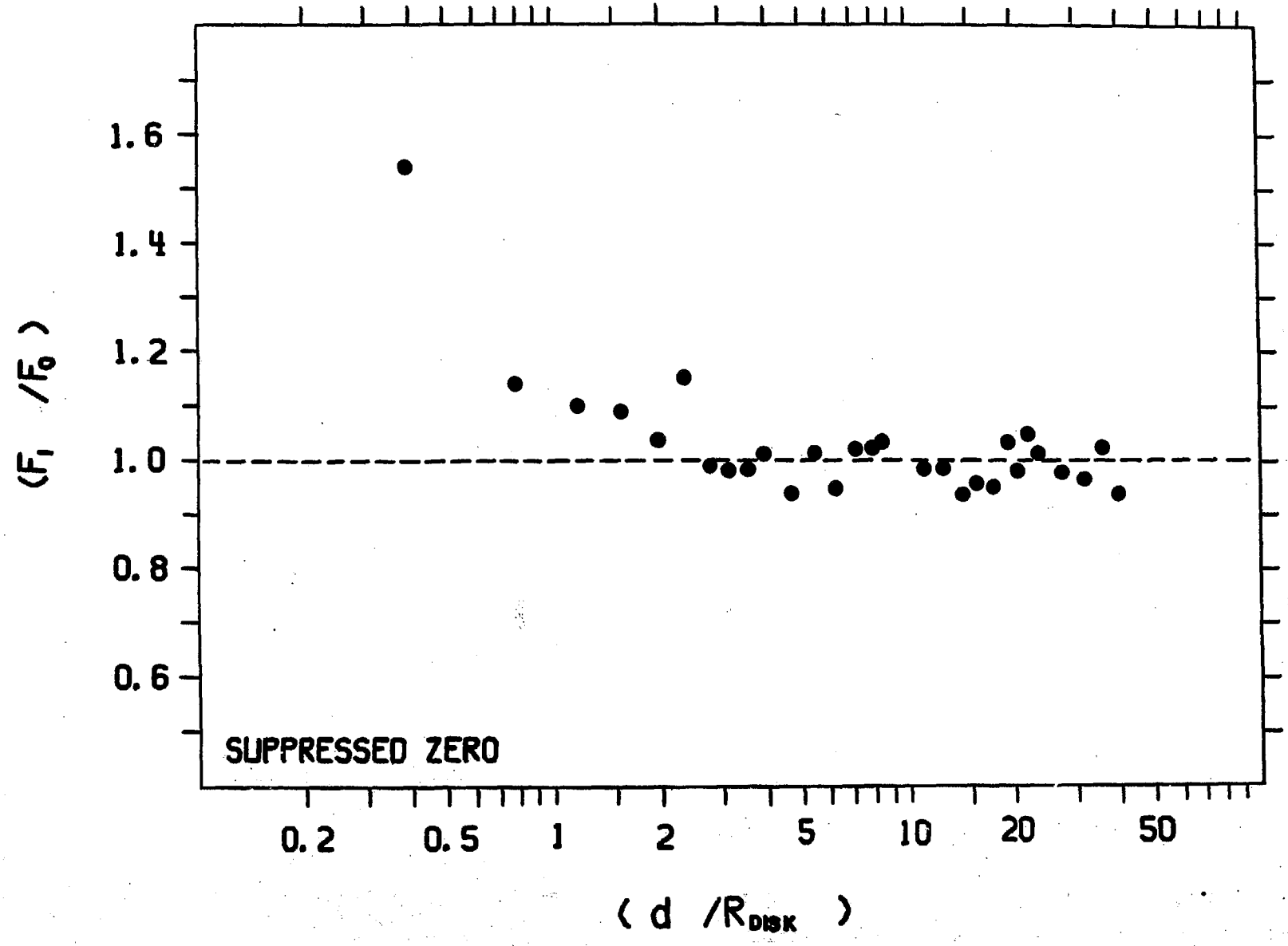

Fig. 6

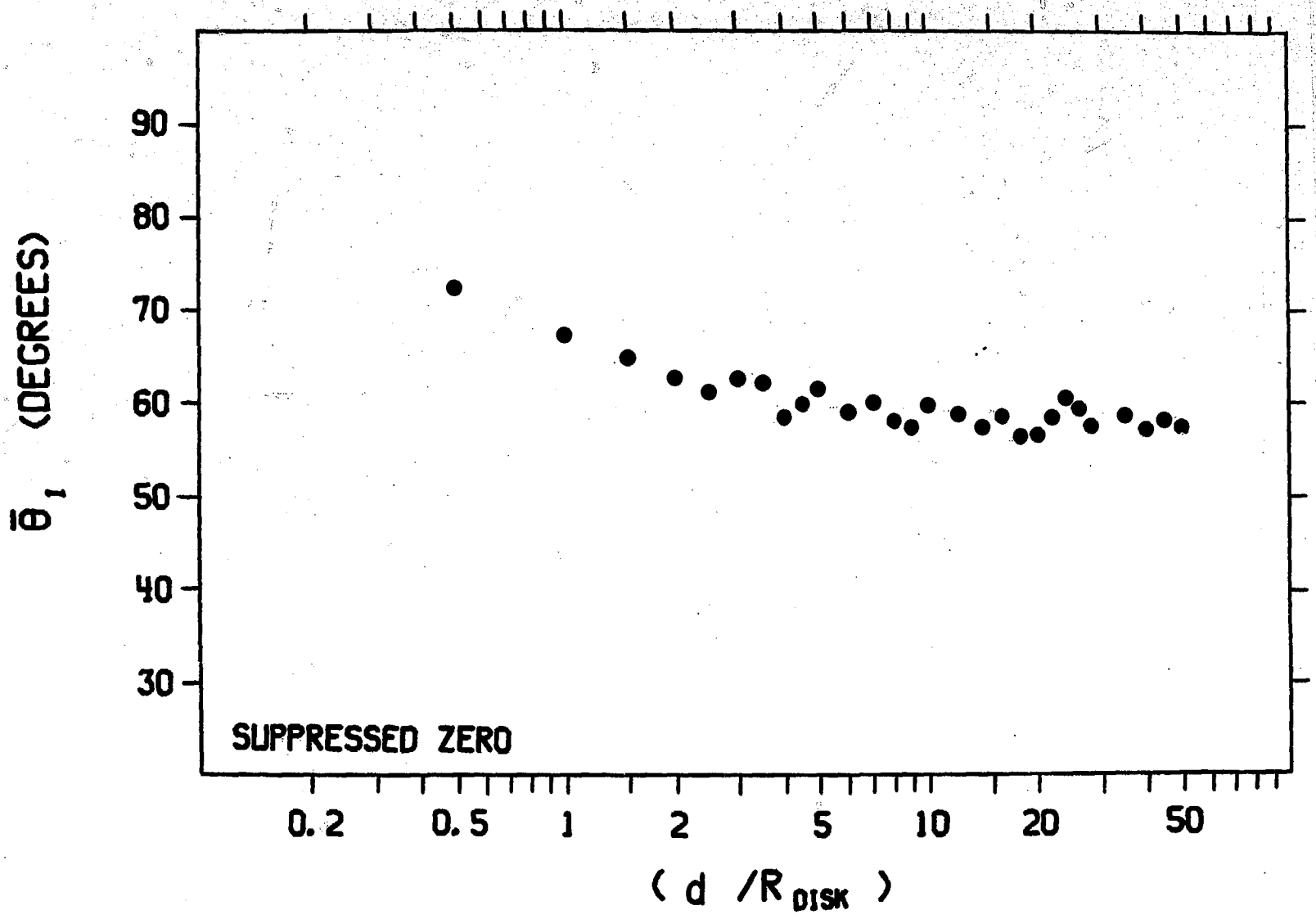
90
80
70
60
50
40
30
$\bar{\theta}_1$ (DEGREES)
SUPPRESSED ZERO
0.2
0.5
1
2
5
10
20
50
(d /R DISK)

Fig. 7

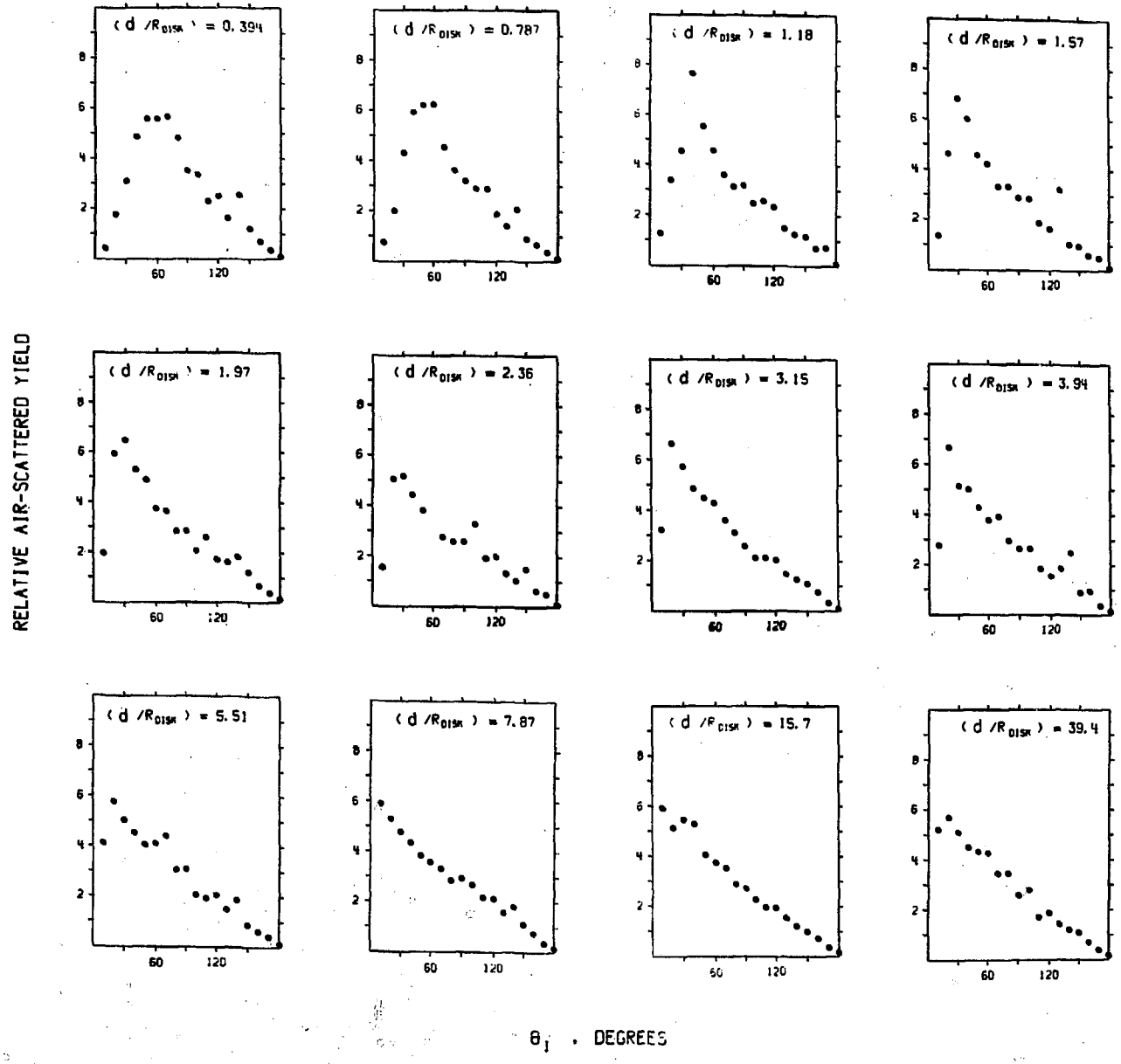
(d /R_DISK) = 0.394
(d /R_DISK) = 0.787
(d /R_DISK) = 1.18
(d /R_DISK) = 1.57
(d /R_DISK) = 1.97
(d /R_DISK) = 2.36
(d /R_DISK) = 3.15
(d /R_DISK) = 3.94
(d /R_DISK) = 5.51
(d /R_DISK) = 7.87
(d /R_DISK) = 15.7
(d /R_DISK) = 39.4
RELATIVE AIR-SCATTERED YIELD
θ_I , DEGREES

Fig. 8

Fig. 9

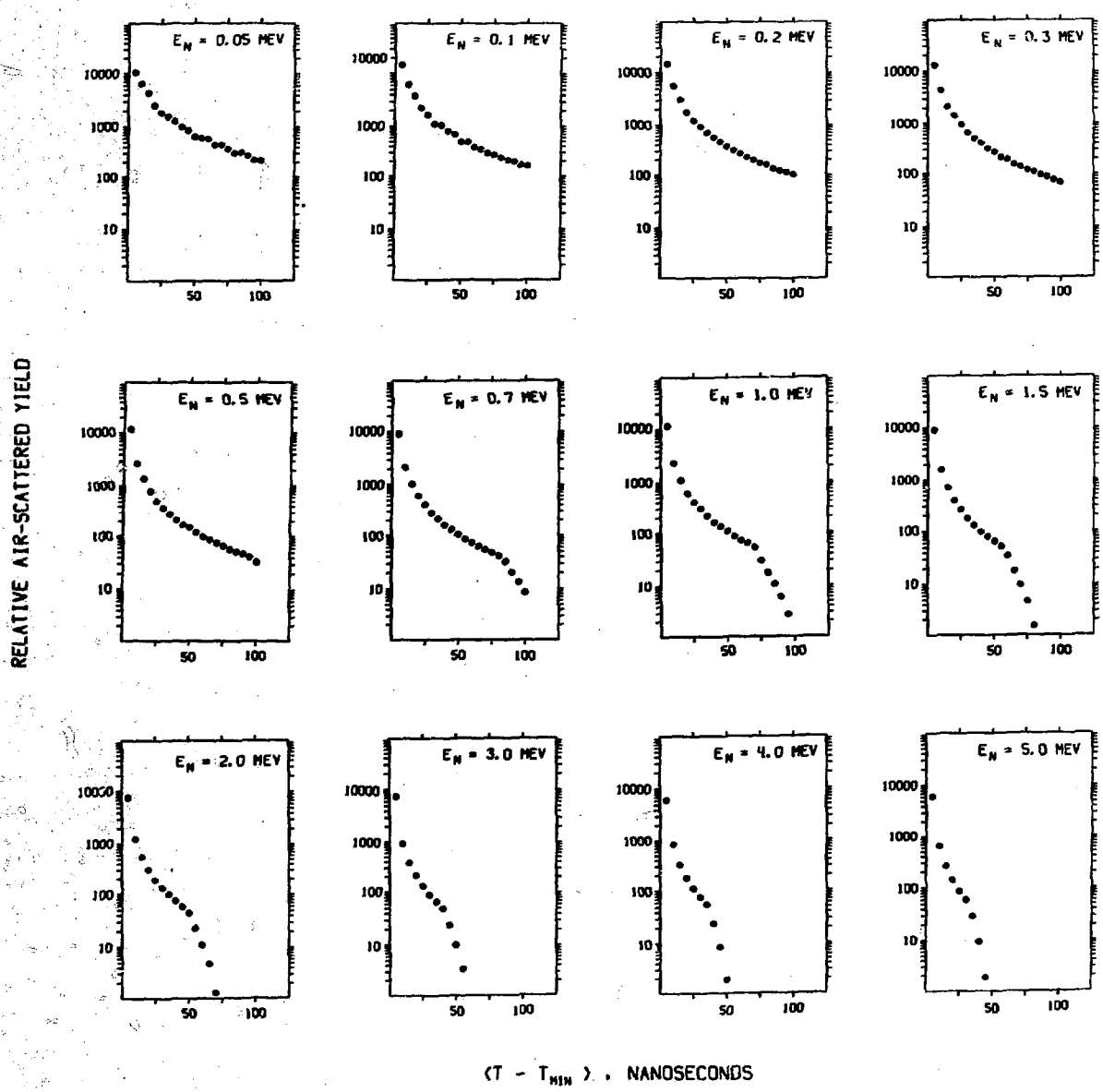
E_N = 0.05 MEV
E_N = 0.1 MEV
E_N = 0.2 MEV
E_N = 0.3 MEV
E_N = 0.5 MEV
E_N = 0.7 MEV
E_N = 1.0 MEV
E_N = 1.5 MEV
E_N = 2.0 MEV
E_N = 3.0 MEV
E_N = 4.0 MEV
E_N = 5.0 MEV
10000
1000
100
10
50
100
RELATIVE AIR-SCATTERED YIELD
$(T - T_{MIN})$, NANOSECONDS

Fig.10

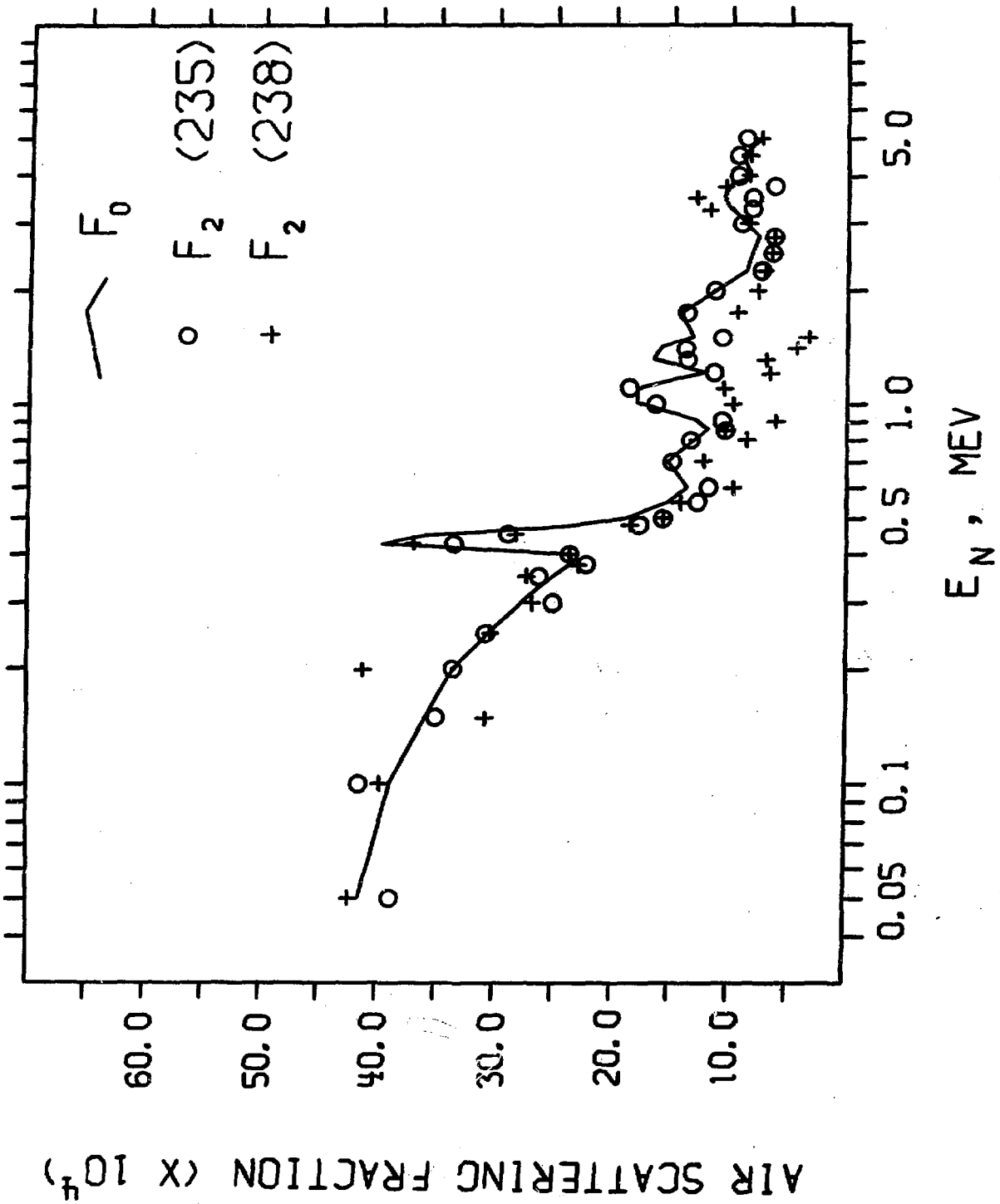
AIR SCATTERING FRACTION (X 10⁴)
60.0
50.0
40.0
30.0
20.0
10.0
0.05
0.1
0.5
1.0
5.0
E_N , MEV
F_0
F_2 (235)
F_2 (238)

Fig.11

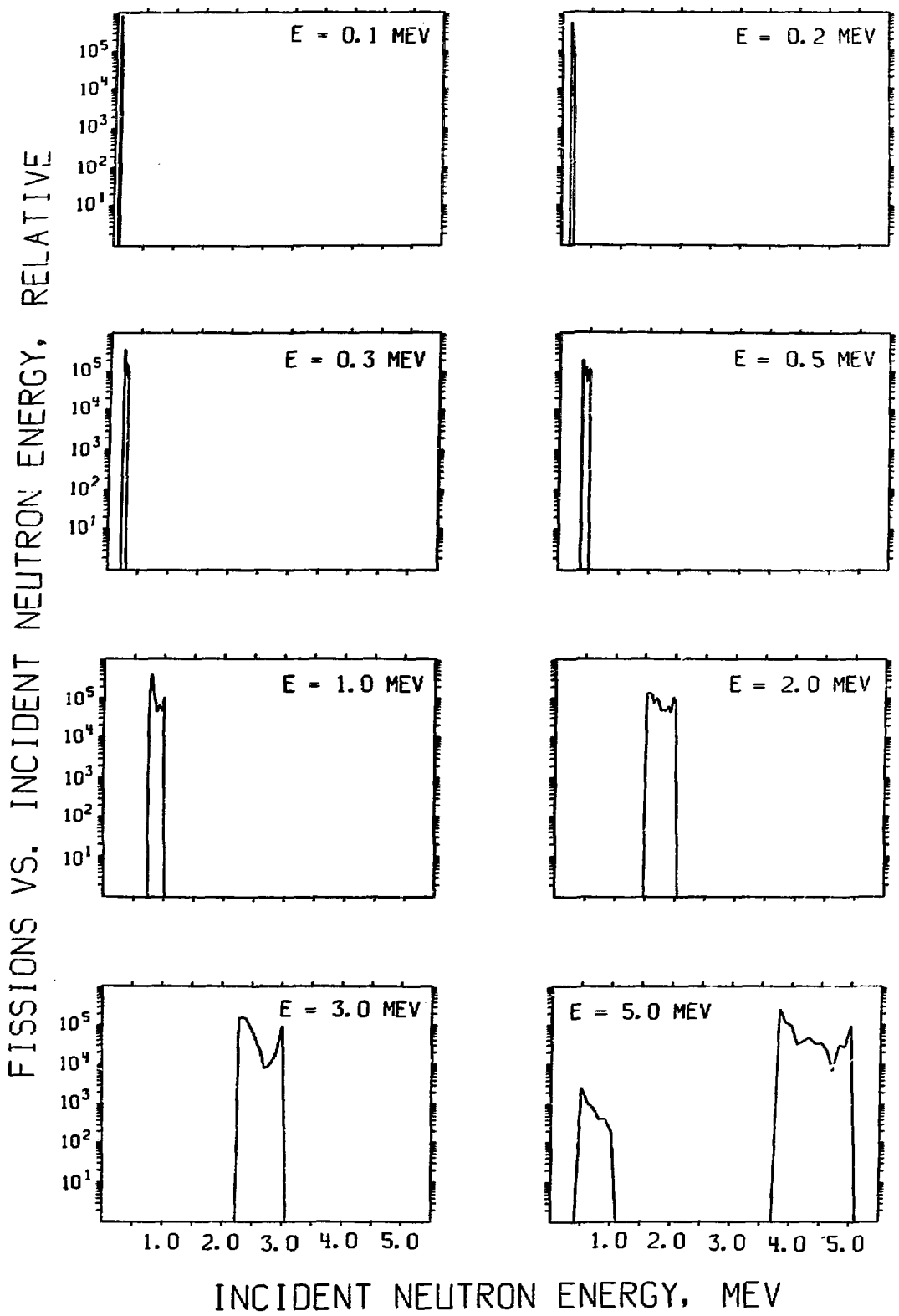
E = 0.1 MEV
E = 0.2 MEV
E = 0.3 MEV
E = 0.5 MEV
E = 1.0 MEV
E = 2.0 MEV
E = 3.0 MEV
E = 5.0 MEV
10^5
10^4
10^3
10^2
10^1
1.0 2.0 3.0 4.0 5.0
FISSIONS VS. INCIDENT NEUTRON ENERGY, RELATIVE
INCIDENT NEUTRON ENERGY, MEV

Fig.12

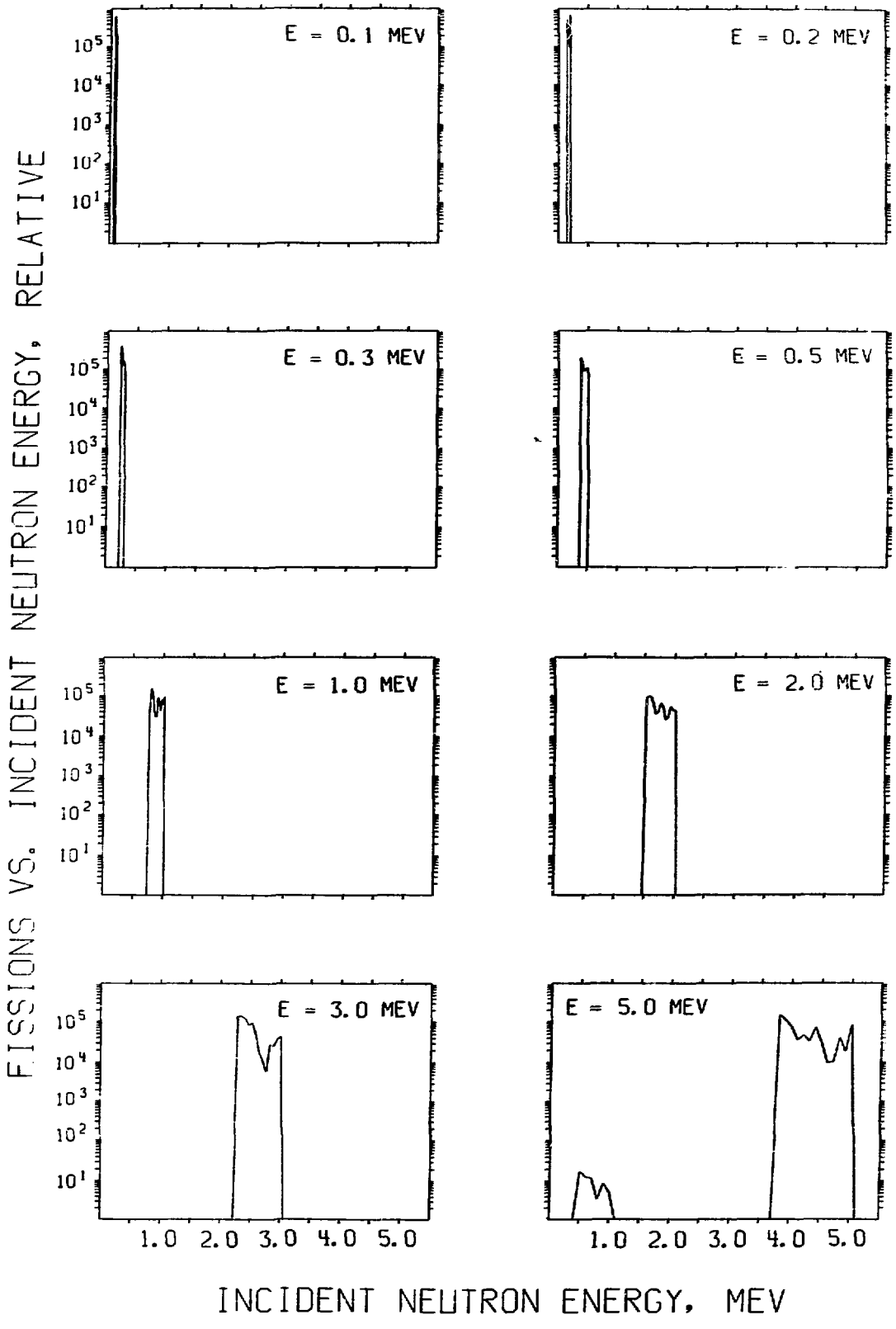
E = 0.1 MEV
E = 0.2 MEV
E = 0.3 MEV
E = 0.5 MEV
E = 1.0 MEV
E = 2.0 MEV
E = 3.0 MEV
E = 5.0 MEV
10^5
10^4
10^3
10^2
10^1
1.0 2.0 3.0 4.0 5.0
FISSIONS VS. INCIDENT NEUTRON ENERGY, RELATIVE
INCIDENT NEUTRON ENERGY, MEV

Fig.13

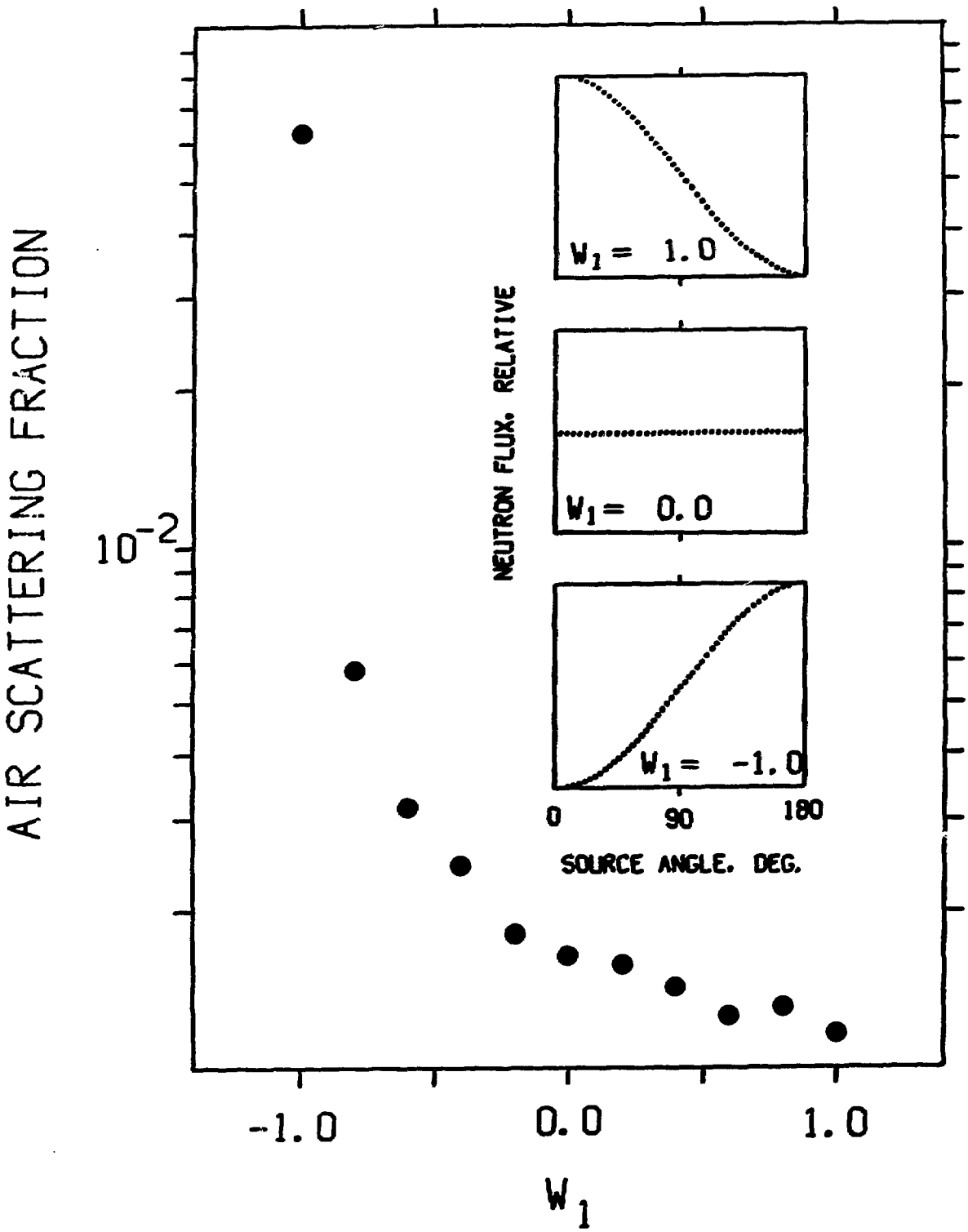
AIR SCATTERING FRACTION
10^{-2}
-1.0
0.0
1.0
W_1
NEUTRON FLUX, RELATIVE
W_1 = 1.0
W_1 = 0.0
W_1 = -1.0
0
90
180
SOURCE ANGLE, DEG.

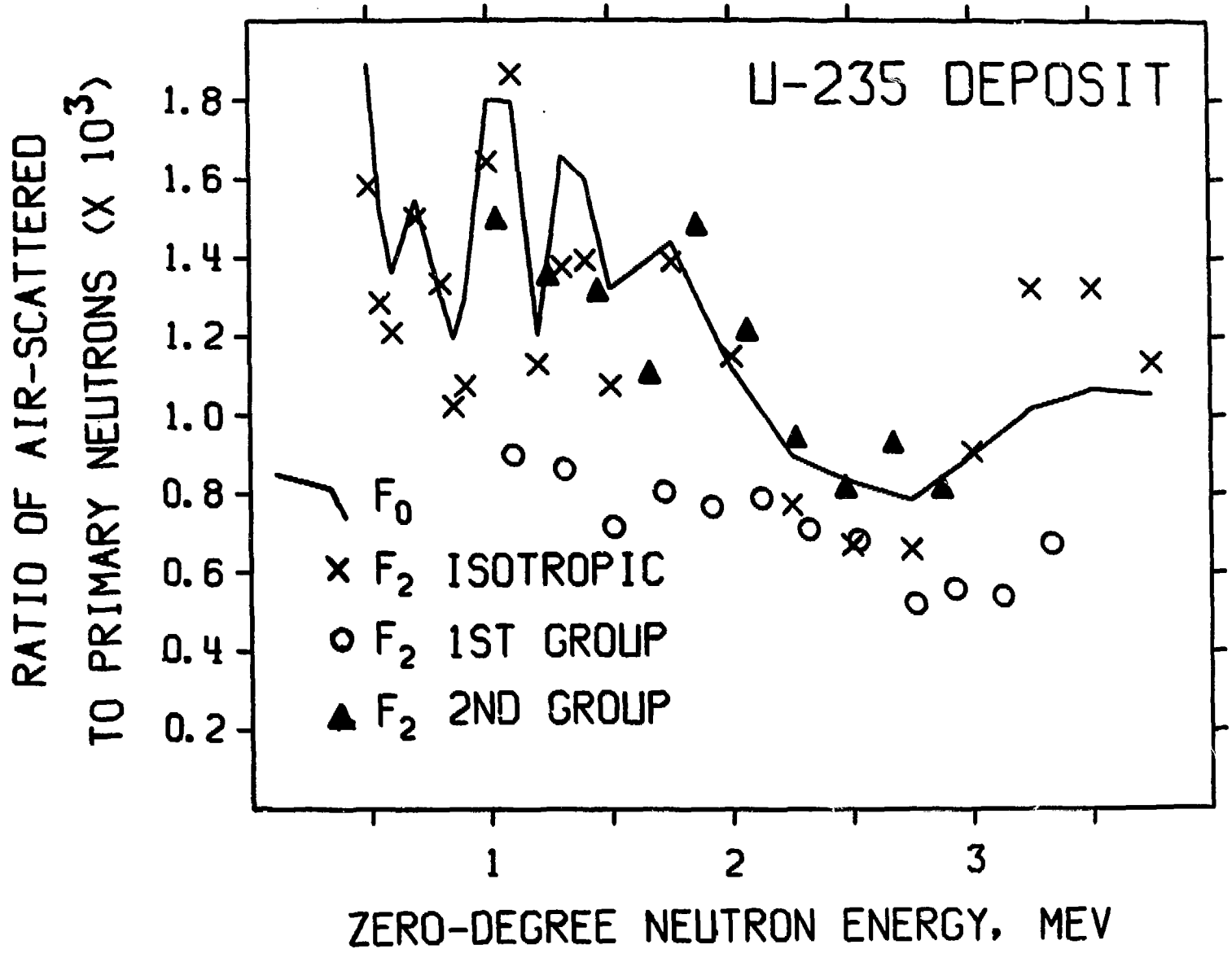
U-235 DEPOSIT
RATIO OF AIR-SCATTERED
TO PRIMARY NEUTRONS (X 10^3)
1.8
1.6
1.4
1.2
1.0
0.8
0.6
0.4
0.2
F0
× F2 ISOTROPIC
○ F2 1ST GROUP
▲ F2 2ND GROUP
1
2
3
ZERO-DEGREE NEUTRON ENERGY, MEV

Fig.14

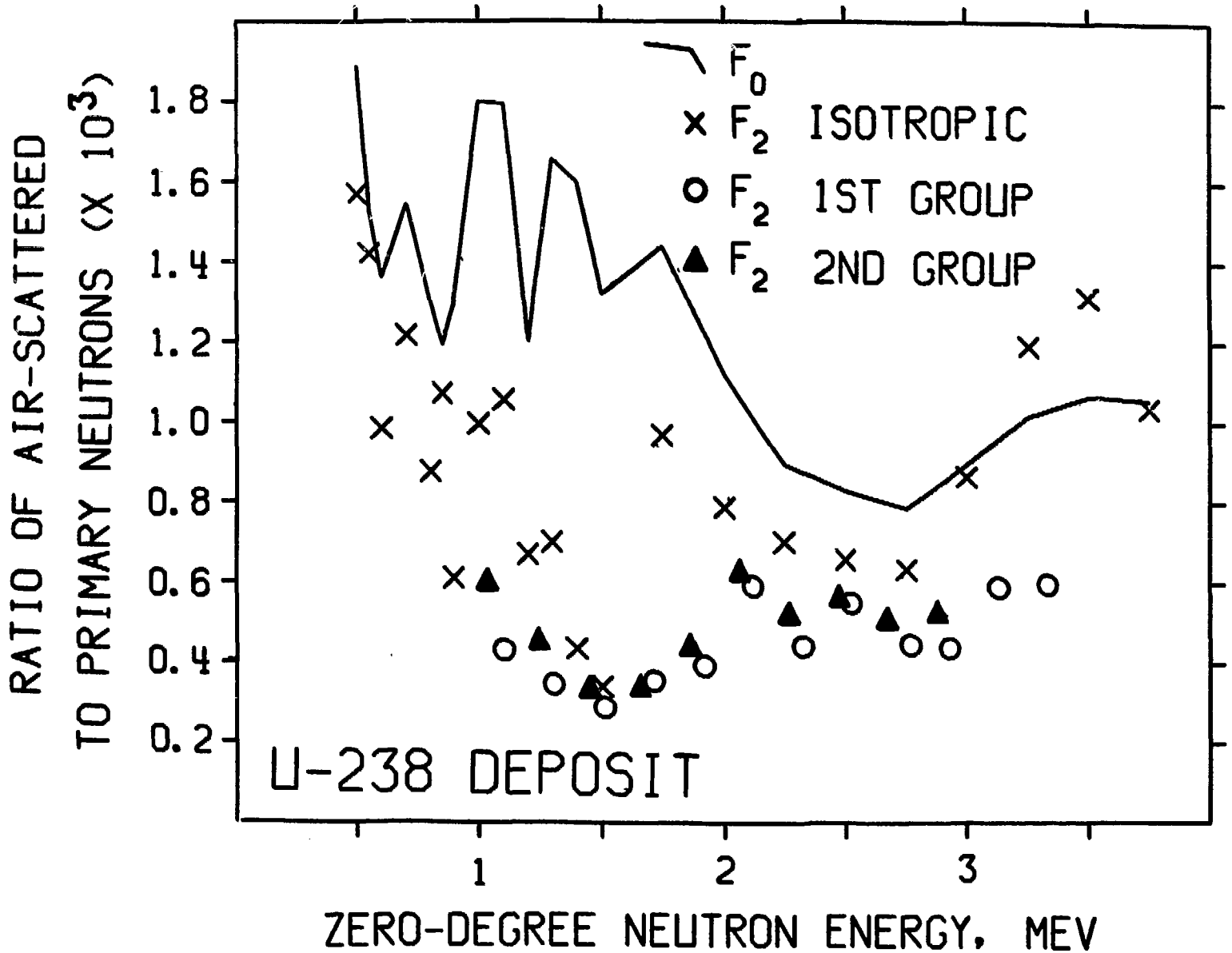
RATIO OF AIR-SCATTERED
TO PRIMARY NEUTRONS (X 10^3)
1.8
1.6
1.4
1.2
1.0
0.8
0.6
0.4
0.2
F0
F2 ISOTROPIC
F2 1ST GROUP
F2 2ND GROUP
U-238 DEPOSIT
1
2
3
ZERO-DEGREE NEUTRON ENERGY, MEV

Fig.15

APPENDIX I

Listing of FORTRAN IV Code AIRSC1

This program was used in conjunction with an SEL 840 MP computer equipped with an extended arithmetic unit to perform the calculations discussed in Section IV. The interpolation tables included in the input provide basic physical data, such as cross sections, which are required for the calculations. Unit 1 refers to a teletype I/O device, Unit 4 is a card reader while Unit 5 is a line printer.

```
C     AIRSC1
C
      DIMENSIØN ENE(50),SIGNE(50),EØE(50),SIGØE(50),THI(36),YSA(36),RANG
     1(36),T(20),YST(21),RTIME(21)
      DATA ATMDN,ATMDØ,AVØG,PI1,PI2/.4034E+20,.1066E+20,.1E-23,3.14159,6
     1.23318/
C
      VALUE(Z,VMIN,VMAX)=VMIN+Z*(VMAX-VMIN)
C
C     CØNTRØL
C
    1 READ(4,2) IC
    2 FØRMAT(I1)
      GØ TØ(10,20,30,40),IC
   10 PAUSE
      GØ TØ 1
C
C     READ INTERPØLATIØN TABLES
C
   20 READ(4,31) NNE
      READ(4,21) (ENE(I),SIGNE(I),I=1,NNE)
   21 FØRMAT(8E10.4)
      READ(4,31) NØE
      READ(4,21) (EØE(I),SIGØE(I),I=1,NØE)
C
C     READ AND WRITE BASIC PARAMETERS
C
   30 READ(4,21) D,RDISK
      READ(4,31) MHIST,NHIST,NTIME,NANG
   31 FØRMAT(16I5)
      READ(4,21) ZAMAX,RAMAX,TRANG
      WRITE(5,35) D,RDISK
   35 FØRMAT(1H1,7HD,RDISK/2E10.4)
      WRITE(5,36) MHIST,NHIST,NTIME,NANG
   36 FØRMAT(22HMHIST,NHIST,NTIME,NANG/4I6)
      WRITE(5,37) ZAMAX,RAMAX,TRANG
   37 FØRMAT(17HZAMAX,RAMAX,TRANG/3E10.4)
      WRITE(5,38)
   38 FØRMAT(/5H.....)
C
C     READ AND WRITE E
C
   40 READ(4,21) E
      WRITE(5,42) E
   42 FØRMAT(1HE/E10.4)
C
C     CALCULATE MACRØSCØPIC ELASTIC SCATTERING CRØSS SECTIØN AND MEAN
C     FREE PATH FØR ELASTIC SCATTERING
C
      CALL INTRPL(NNE,ENE,SIGNE,E,VSNE)
      CALL INTRPL(NØE,EØE,SIGØE,E,VSØE)
      SIGME=AVØG*(ATMDN*VSNE+ATMDØ*VSØE)
      FREE=1.0/SIGME
C
C     CALCULATE INCIDENT ANGLES THI(I)
C
      DØ 48 I=1,NANG
   48 THI(I)=180.0*FLØAT(I)/FLØAT(NANG)
C
```

```
C       CALCULATE T(I) AND TMIN
C
        DØ 50 I=1,NTIME
   50   T(I)=TRANG*FLØAT(I)/FLØAT(NTIME)
        TMIN=TIME(E,D)
C
C.....CALCULATE YDIR
C
        YDIR=0.0
        DØ 100 IDIR=1,MHIST
C
C       SELECT RF AT RANDØM
C
        Z=RANF(-1)
        RF=VALUE(Z,0.0,RDISK)
C
C       CALCULATE THS AND DO
C
        THS=ATAN(RF/D)
        DO=D/CØS(THS)
C
  100   YDIR=YDIR+(RF/DO/DO)
C
C       CALCULATE HISTØRY AVERAGE
C
        YDIR=YDIR/FLØAT(MHIST)
C
C......CALCULATE YSA(I) AND YST(I)
C
        DØ 105 I=1,NANG
  105   YSA(I)=0.0
        NBIN=NTIME+1
        DØ 110 I=1,NBIN
  110   YST(I)=0.0
        SUMNTH=0.0
        SUMD=0.0
C
        DØ 900 ISCAT=1,NHIST
C
C       SELECT RF,RA,ZA AND PHA AT RANDØM
C
        Z=RANF(-1)
        RF=VALUE(Z,0.0,RDISK)
        Z=RANF(-1)
        RA=VALUE(Z,0.0,RAMAX)
        Z=RANF(-1)
        ZA=VALUE(Z,-ZAMAX,ZAMAX)
        Z=RANF(-1)
        PHA=VALUE(Z,0.0,PI2)
C
C       CALCULATE XA,YA,D1 AND D2. SKIP TRIAL IF D1 ØR D2 TØØ SMALL
C
        XA=RA*CØS(PHA)
        YA=RA*SIN(PHA)
        D1=SQRT(XA*XA+YA*YA+(ZA-D)*(ZA-D))
        IF(D1-.1E-10) 900,900,120
  120   D2=SQRT((XA-RF)*(XA-RF)+YA*YA+ZA*ZA)
        IF(D2-.1E-10) 900,900,130
C
C       CALCULATE THINC AND INDXA
```

```
C
  130 CALL ANGLE(0.,0.,0.,0.,0.,D,RF,0.,0.,XA,YA,ZA,THINC)
      THINC=57.2957795*THINC
      INDXA=THINC*FLØAT(NANG)/180.001
      INDXA=INDXA+1
C
C     CALCULATE T1,T2 AND INDXT
C
      T1=TIME(E,D1)
      T2=TIME(E,D2)
      INDXT=(T1+T2-TMIN)*FLØAT(NTIME)/TRANG
      INDXT=INDXT+1
      IF(INDXT.GT.NBIN) INDXT=NBIN
C
      YLD=RA*RF/D1/D1/D2/D2
      SUMNTH=SUMNTH+YLD*THINC
      SUMD=SUMD+YLD
      YSA(INDXA)=YSA(INDXA)+YLD
      YST(INDXT)=YST(INDXT)+YLD
  900 CØNTINUE
C
C     MULTIPLY BY SIGME AND AIR PARAMETER SPACE VØLUME. CALCULATE
C     HISTØRY AVERAGES
C
      DØ 905 I=1,NANG
  905 YSA(I)=RAMAX*ZAMAX*SIGME*YSA(I)/FLØAT(NHIST)
      DØ 910 I=1,NBIN
  910 YST(I)=RAMAX*ZAMAX*SIGME*YST(I)/FLØAT(NHIST)
      THINCV=SUMNTH/SUMD
C
C     CALCULATE RANG(I),RTIME(I),TØTRAT,FT1 AND FT2
C
      DØ 920 I=1,NANG
  920 RANG(I)=YSA(I)/YDIR
      TØTRAT=0.0
      DØ 1000 I=1,NBIN
      RTIME(I)=YST(I)/YDIR
 1000 TØTRAT=TØTRAT+RTIME(I)
      FT2=RTIME(NBIN)/TØTRAT
      FT1=1.0-FT2
C
C     WRITE RESULTS
C
      WRITE(5,1900) YDIR
 1900 FØRMAT(4HYDIR/E10.4)
      WRITE(5,2000) TMIN,FREE
 2000 FØRMAT(9HTMIN,FREE/2E10.4)
      WRITE(5,2400)
 2400 FØRMAT(6HTHI(I))
      WRITE(5,3000) (THI(I),I=1,NANG)
      WRITE(5,2401)
 2401 FØRMAT(7HRANG(I))
      WRITE(5,3000) (RANG(I),I=1,NANG)
      WRITE(5,2001)
 2001 FØRMAT(4HT(I))
      WRITE(5,3000) (T(I),I=1,NTIME)
 3000 FØRMAT(4E10.4)
      WRITE(5,2002)
 2002 FØRMAT(8HRTIME(I))
      WRITE(5,3000) (RTIME(I),I=1,NBIN)
```

```
      WRITE(5,2003) TØTRAT,FT1,FT2
 2003 FØRMAT(14HTØTRAT,FT1,FT2/3E10.4)
      WRITE(5,2004) THINCV
 2004 FØRMAT(6HTHINCV/E10.4)
      WRITE(5,2005)
 2005 FØRMAT(/5H-----)
C
      GØ TØ 1
      END
      FUNCTIØN TIME(EIN,R)
      E=EIN/939.549
      V=(4.2997925E+11)*SQRT(1.0-(1.0/(E+1.0)/(E+1.0)))
      TIME=R/V
      RETURN
      END
      SUBRØUTINE ANGLE(X1H,Y1H,Z1H,X1T,Y1T,Z1T,X2H,Y2H,Z2H,X2T,Y2T,Z2T,T
     1H)
      V1=SQRT((X1H-X1T)*(X1H-X1T)+(Y1H-Y1T)*(Y1H-Y1T)+(Z1H-Z1T)*(Z1H-Z1T
     1))
      V2=SQRT((X2H-X2T)*(X2H-X2T)+(Y2H-Y2T)*(Y2H-Y2T)+(Z2H-Z2T)*(Z2H-Z2T
     1))
      DØT=(X1H-X1T)*(X2H-X2T)+(Y1H-Y1T)*(Y2H-Y2T)+(Z1H-Z1T)*(Z2H-Z2T)
      CTH=DØT/V1/V2
      TH=ARCCØS(CTH,2)
      RETURN
      END
      FUNCTIØN ARCCØS(X,K)
      ARCCØS=1.5707963
      IF(X*X.GT.1.0E-70) ARCCØS=ATAN(SQRT(1./X/X-1.))
      IF(X.LT.0.) ARCCØS=3.1415926-ARCCØS
      GØ TØ (100,200),K
  100 ARCCØS=ARCCØS*57.2957795
  200 RETURN
      END
      SUBRØUTINE INTRPL(N,XT,YT,X,Y)
      DIMENSIØN XT(N),YT(N)
      IF(X-XT(1)) 1,3,4
    1 WRITE(1,2)
    2 FØRMAT(8HRANG ERR)
      PAUSE
    3 Y=YT(1)
      GØ TØ 24
    4 IF(X-XT(N)) 7,5,1
    5 Y=YT(N)
      GØ TØ 24
    7 I=0
      J=N
    8 K=0.5*FLØAT(J-I)+0.1
      K=K+I
      IF(X-XT(K)) 9,10,11
    9 J=K
      GØ TØ 12
   10 Y=YT(K)
      GØ TØ 24
   11 I=K
   12 IF(J-I-1) 13,13,8
   13 I=J
      J=I-1
      DEN=XT(J)-XT(I)
      C1=(XT(J)*YT(I)-XT(I)*YT(J))/DEN
```

```
      C2=(YT(J)-YT(I))/DEN
      Y=C1+C2*X
   24 RETURN
      END
$
```

APPENDIX II

Listing of FORTRAN IV Program AIRSC2

This program was used in conjunction with an SEL 840 MP computer equipped with an extended arithmetic unit to perform the calculations discussed in Section V. The interpolation tables included in the input provide basic physical data, such as cross sections, which are required for the calculations. Unit 1 refers to a teletype I/O device, Unit 4 is a card reader (or punch for output) while Unit 5 is a line printer.

```
C     AIRSC2
C
      DIMENSIØN WS(5),ATMU(4),NUT(4),EUT(4,20),SIGUT(4,20),NUF(4),EUF(4,
     150),SIGUF(4,50),ENT(50),SIGNT(50),ENE(50),SIGNE(50),NWNE(5),EWNE(5
     2,30),WNE(5,30),QNI(3),NNI(3),ENI(3,20),SIGNI(3,20),EØT(50),SIGØT(5
     30),EØE(50),SIGØE(50),NWØE(5),EWØE(5,30),WØE(5,30),QØI(3),NØI(3),EØ
     4I(3,20),SIGØI(3,20),T(20),YSCAT(21),RATIØ(21),THIC(36),YSANG(36),R
     5ANG(36),ENER(100),YSEN(100),REN(100),A(50),B(50),WØRK(50)
      DATA ATMDN,ATMDØ,AVØG,PI1,PI2/.4034E+20,.1066E+20,.1E-23,3.14159,6
     1.28318/
C
      VALUE(Z,VMIN,VMAX)=VMIN+Z*(VMAX-VMIN)
C
C     CØNTRØL
C
    1 READ(4,2) IC
    2 FØRMAT(I1)
      GØ TØ(10,20,30,40),IC
   10 PAUSE
      GØ TØ 1
C
C     READ INTERPØLATIØN TABLES
C
   20 DØ 22 I=1,4
      READ(4,21) NUT(I)
   21 FØRMAT(16I5)
      N=NUT(I)
   22 READ(4,23) (EUT(I,J),SIGUT(I,J),J=1,N)
   23 FØRMAT(8E10.4)
      DØ 231 I=1,4
      READ(4,21) NUF(I)
      N=NUF(I)
  231 READ(4,23) (EUF(I,J),SIGUF(I,J),J=1,N)
      READ(4,21) NNT
      READ(4,23) (ENT(I),SIGNT(I),I=1,NNT)
      READ(4,21) NNE
      READ(4,23) (ENE(I),SIGNE(I),I=1,NNE)
      DØ 24 I=1,5
      READ(4,21) NWNE(I)
      N=NWNE(I)
   24 READ(4,23) (EWNE(I,J),WNE(I,J),J=1,N)
      READ(4,21) MNI
      IF(MNI.EQ.0) GØ TØ 26
      READ(4,23) (QNI(I),I=1,MNI)
      DØ 25 I=1,MNI
      READ(4,21) NNI(I)
      N=NNI(I)
   25 READ(4,23) (ENI(I,J),SIGNI(I,J),J=1,N)
   26 READ(4,21) NØT
      READ(4,23) (EØT(I),SIGØT(I),I=1,NØT)
      READ(4,21) NØE
      READ(4,23) (EØE(I),SIGØE(I),I=1,NØE)
      DØ 27 I=1,5
      READ(4,21) NWØE(I)
      N=NWØE(I)
   27 READ(4,23) (EWØE(I,J),WØE(I,J),J=1,N)
      READ(4,21) MØI
      IF(MØI.EQ.0) GØ TØ 30
      READ(4,23) (QØI(I),I=1,MØI)
```

```
      DØ 28 I=1,MØI
      READ(4,21) NØI(I)
      N=NØI(I)
   28 READ(4,23) (EØI(I,J),SIGØI(I,J),J=1,N)
C
C     READ AND WRITE BASIC PARAMETERS
C
   30 READ(4,21) MHIST,NHISTL,NTIME,NANG,NENR
      READ(4,23) ZAMAX,RAMAX
      READ(4,23) D,RDISK
      READ(4,23) (ATMU(I),I=1,4)
      READ(4,23) TRANG
      READ(4,23) A1,A2,QS
      WRITE(5,31) MHIST,NHISTL,NTIME,NANG,NENR
   31 FØRMAT(1H1,28HMHIST,NHISTL,NTIME,NANG,NENR/5I6)
      WRITE(5,32) ZAMAX,RAMAX
   32 FØRMAT(11HZAMAX,RAMAX/2E10.4)
      WRITE(5,33) D,RDISK
   33 FØRMAT(7HD,RDISK/2E10.4)
      WRITE(5,34)
   34 FØRMAT(7HATMU(I))
      WRITE(5,23) (ATMU(I),I=1,4)
      WRITE(5,35) TRANG
   35 FØRMAT(5HTRANG/E10.4)
      WRITE(5,36) A1,A2,QS
   36 FØRMAT(8HA1,A2,QS/3E10.4)
      WRITE(5,37)
   37 FØRMAT(/5H.....)
C
C     READ AND WRITE VARIABLE PARAMETERS
C
   40 READ(4,41) E1,NWS
   41 FØRMAT(E10.4,I5)
      IF(NWS.GT.0) READ(4,23) (WS(I),I=1,NWS)
      WRITE(5,42) E1,NWS
   42 FØRMAT(/6HE1,NWS/E10.4,I5)
      IF(NWS.EQ.0) GØ TØ 50
      WRITE(5,43)
   43 FØRMAT(5HWS(I))
      WRITE(5,23) (WS(I),I=1,NWS)
C
C     CALCULATE T(I)
C
   50 DØ 51 I=1,NTIME
   51 T(I)=TRANG*FLØAT(I)/FLØAT(NTIME)
C
C     CALCULATE THIC(I)
C
      DØ 52 I=1,NANG
   52 THIC(I)=180.0*FLØAT(I)/FLØAT(NANG)
C
C     CALCULATE FLIGHT TIME SPREAD FØR DIRECT EVENTS,ENMAX AND ENER(I)
C
      THS=ATAN(RDISK/D)
      D0=D/CØS(THS)
      CALL KINAM(A1,A2,1.0087,QS,E1,THS,EN0,EDUM)
      TMAX=TIME(EN0,D0)
      CALL KINAM(A1,A2,1.0087,QS,E1,0.0,EN0,EDUM)
      ENMAX=1.00001*EN0
      TMIN=TIME(EN0,D)
```

```
      DT=TMAX-TMIN
      DØ 53 I=1,NENR
   53 ENER(I)=ENMAX*FLØAT(I)/FLØAT(NENR)
C
C     CALCULATE ZERØ-DEGREE MEAN FREE PATH
C
      CALL INTRPL(NNT,ENT,SIGNT,ENO,VSNT)
      CALL INTRPL(NØT,EØT,SIGØT,ENO,VSØT)
      SIGAIR=AVØG*(ATMDN*VSNT+ATMDØ*VSØT)
      FREE=1.0/SIGAIR
C
C.....CALCULATE YDIR
C
      YDIR=0.0
      DØ 100 IDIR=1,MHIST
C
C     SELECT RF AT RANDØM
C
      Z=RANF(-1)
      RF=VALUE(Z,0.0,RDISK)
C
C     CALCULATE THS,DO AND ENO
C
      THS=ATAN(RF/D)
      CS=CØS(THS)
      DO=D/CS
      CALL KINAM(A1,A2,1.0087,QS,E1,THS,ENO,EDUM)
C
C     CALCULATE SØURCE FLUX
C
      CALL DISTR(NWS,WS,THS,FS)
C
C     CALCULATE ATTNO
C
      CALL INTRPL(NNT,ENT,SIGNT,ENO,VSNT)
      CALL INTRPL(NØT,EØT,SIGØT,ENO,VSØT)
      SIGAIR=AVØG*(ATMDN*VSNT+ATMDØ*VSØT)
      ATTNO=EXF(-SIGAIR*DO)
C
C     CALCULATE FUT AND FUF
C
      FUT=0.0
      DØ 61 I=1,4
      N=NUT(I)
      DØ 60 J=1,N
      A(J)=EUT(I,J)
   60 B(J)=SIGUT(I,J)
      CALL INTRPL(N,A,B,ENO,VSUT)
   61 FUT=FUT+ATMU(I)*VSUT
      FUT=FUT*AVØG
      FUF=0.0
      DØ 63 I=1,4
      N=NUF(I)
      DØ 62 J=1,N
      A(J)=EUF(I,J)
   62 B(J)=SIGUF(I,J)
      CALL INTRPL(N,A,B,ENO,VSUF)
   63 FUF=FUF+ATMU(I)*VSUF
      FUF=FUF*AVØG
C
```

```
  100 YDIR=YDIR+(FS*CS*ATTN0*RF*FUF*TRANS(FUT,PI1,RDISK,CS)/D0/D0/FUT)
C
C     CALCULATE HISTØRY AVERAGE
C
      YDIR=YDIR/FLØAT(MHIST)
C
C.....CALCULATE YSCAT(I),YSANG(I) AND YSEN(I)
C
      NBIN=NTIME+1
      DØ 110 I=1,NBIN
  110 YSCAT(I)=0.0
      DØ 111 I=1,NANG
  111 YSANG(I)=0.0
      DØ 112 I=1,NENR
  112 YSEN(I)=0.0
      SUMNE=0.0
      SUMNTH=0.0
      SUMD=0.0
C
      NHIST=0
  113 CØNTINUE
      NHIST=NHIST+1
C
C     SELECT RF,RA,ZA AND PHA AT RANDØM
C
      Z=RANF(-1)
      RF=VALUE(Z,0.0,RDISK)
      Z=RANF(-1)
      RA=VALUE(Z,0.0,RAMAX)
      Z=RANF(-1)
      ZA=VALUE(Z,-ZAMAX,ZAMAX)
      Z=RANF(-1)
      PHA=VALUE(Z,0.0,PI2)
C
C     CALCULATE XA,YA,D1 AND D2. SKIP TRIAL IF D1 ØR D2 TØØ SMALL
C
      XA=RA*CØS(PHA)
      YA=RA*SIN(PHA)
      D1=SQRT(ABS(XA*XA+YA*YA+(ZA-D)*(ZA-D)))
      IF((D1/D)-.1E-05) 113,113,120
  120 D2=SQRT(ABS((XA-RF)*(XA-RF)+YA*YA+ZA*ZA))
      IF((D2/D)-.1E-05) 113,113,130
C
C     CALCULATE THS,EN1 AND T1
C
  130 CALL ANGLE(0.,0.,0.,0.,0.,D,XA,YA,ZA,0.,0.,D,THS)
      CALL KINAM(A1,A2,1.0087,QS,E1,THS,EN1,EDUM)
      T1=TIME(EN1,D1)
C
C     CALCULATE SØURCE FLUX
C
      CALL DISTR(NWS,WS,THS,FS)
C
C     CALCULATE ATTN1
C
      CALL INTRPL(NNT,ENT,SIGNT,EN1,VSNT)
      CALL INTRPL(NØT,EØT,SIGØT,EN1,VSØT)
      SIGAIR=AVØG*(ATMDN*VSNT+ATMDØ*VSØT)
      ATTN1=EXF(-SIGAIR*D1)
C
```

```
C       CALCULATE THA,THI,THINC AND JNDEX. SKIP TRIAL IF THINC TØØ CLØSE
C       TØ 90 DEGREES
C
        CALL ANGLE(RF,C.,0.,XA,YA,ZA,XA,YA,ZA,0.,0.,D,THA)
        CALL ANGLE(0.,0.,0.,0.,0.,D,RF,0.,0.,XA,YA,ZA,THI)
        CI=ABS(CØS(THI))
        THINC=57.2957795*THI
        IF(ABS(THINC-90.0)-0.01) 113,113,131
  131   JNDEX=THINC*FLØAT(NANG)/180.001
        JNDEX=JNDEX+1
C
CXX     CØNTRIBUTIØN FRØM NITRØGEN ELASTIC SCATTERING
C
C       CALCULATE EN2,T2,INDEX AND KNDEX
C
        CALL KINAM(1.0087,14.003,1.0087,0.,EN1,THA,EN2,EDUM)
        KNDEX=EN2*FLØAT(NENR)/ENMAX
        KNDEX=KNDEX+1
        T2=TIME(EN2,D2)
        INDEX=(T1+T2-TMIN)*FLØAT(NTIME)/TRANG
        INDEX=INDEX+1
        IF(INDEX.GT.NBIN) INDEX=NBIN
C
C       DETERMINE NØRMALIZED NITRØGEN DIFFERENTIAL ELASTIC SCATTERING
C       CRØSS SECTIØN
C
        CALL INTRPL(NNE,ENE,SIGNE,EN1,VSNE)
        DØ 141 I=1,5
        N=NWNE(I)
        DØ 140 J=1,N
        A(J)=ENNE(I,J)
  140   B(J)=WNE(I,J)
  141   CALL INTRPL(N,A,B,EN1,WØRK(I))
        CALL NØRM(WØRK,CØNST)
        CALL DISTR(5,WØRK,THA,S1)
        DESN=CØNST*VSNE*S1*AVØG/PI2/2.0
C
C       CALCULATE ATTN2
C
        CALL INTRPL(NNT,ENT,SIGNT,EN2,VSNT)
        CALL INTRPL(NØT,EØT,SIGØT,EN2,VSØT)
        SIGAIR=AVØG*(ATMDN*VSNT+ATMDØ*VSØT)
        ATTN2=EXP(-SIGAIR*D2)
C
C       CALCULATE FUT AND FUF
C
        FUT=0.0
        DØ 151 I=1,4
        N=NUT(I)
        DØ 150 J=1,N
        A(J)=EUT(I,J)
  150   B(J)=SIGUT(I,J)
        CALL INTRPL(N,A,B,EN2,VSUT)
  151   FUT=FUT+ATMU(I)*VSUT
        FUT=FUT*AVØG
        FUF=0.0
        DØ 153 I=1,4
        N=NUF(I)
        DØ 152 J=1,N
        A(J)=EUF(I,J)
```

```
  152 B(J)=SIGUF(I,J)
      CALL INTRPL(N,A,B,EN2,VSUF)
  153 FUF=FUF+ATMU(I)*VSUF
      FUF=FUF*AVØG
C
      YLD=FS*CI*ATTN1*ATTN2*RF*RA*ATMDN*DESN*FUF*TRANS(FUT,PI1,RDISK,CI)
     1/D1/D1/D2/D2/FUT
      SUMNE=SUMNE+YLD*EN2
      SUMNTH=SUMNTH+YLD*THINC
      SUMD=SUMD+YLD
      YSCAT(INDEX)=YSCAT(INDEX)+YLD
      YSANG(JNDEX)=YSANG(JNDEX)+YLD
      YSEN(KNDEX)=YSEN(KNDEX)+YLD
C
CXX   CØNTRIBUTIØN FRØM NITRØGEN INELASTIC SCATTERING
C
      IF(MNI.EQ.0) GØ TØ 209
      DØ 200 INI=1,MNI
C
C     CHECK IF REACTIØN IS ENERGETICALLY ALLØWED. CALCULATE T2,INDEX
C     AND KNDEX
C
      CALL KINAM(1.0087,14.003,1.0087,QNI(INI),EN1,THA,EN2,EDUM)
      IF(EN2) 200,200,160
  160 T2=TIME(EN2,D2)
      KNDEX=EN2*FLØAT(NENR)/ENMAX
      KNDEX=KNDEX+1
      INDEX=(T1+T2-TMIN)*FLØAT(NTIME)/TRANG
      INDEX=INDEX+1
      IF(INDEX.GT.NBIN) INDEX=NBIN
C
C     DETERMINE NØRMALIZED NITRØGEN DIFFERENTIAL INELASTIC SCATTERING
C     CRØSS SECTIØN (ISØTRØPIC)
C
      N=NNI(INI)
      DØ 161 J=1,N
      A(J)=ENI(INI,J)
  161 B(J)=SIGNI(INI,J)
      CALL INTRPL(N,A,B,EN1,VSNI)
      DISN=VSNI*AVØG/PI2/2.0
C
C     CALCULATE ATTN2
C
      CALL INTRPL(NNT,ENT,SIGNT,EN2,VSNT)
      CALL INTRPL(NØT,EØT,SIGØT,EN2,VSØT)
      SIGAIR=AVØG*(ATMDN*VSNT+ATMDØ*VSØT)
      ATTN2=EXF(-SIGAIR*D2)
C
C     CALCULATE FUT AND FUF
C
      FUT=0.0
      DØ 163 I=1,4
      N=NUT(I)
      DØ 162 J=1,N
      A(J)=EUT(I,J)
  162 B(J)=SIGUT(I,J)
      CALL INTRPL(N,A,B,EN2,VSUT)
  163 FUT=FUT+ATMU(I)*VSUT
      FUT=FUT*AVØG
      FUF=0.0
```

```
      DØ 165 I=1,4
      N=NUF(I)
      DØ 164 J=1,N
      A(J)=EUF(I,J)
  164 B(J)=SIGUF(I,J)
      CALL INTRPL(N,A,B,EN2,VSUF)
  165 FUF=FUF+ATMU(I)*VSUF
      FUF=FUF*AVØG
C
      YLD=FS*CI*ATTN1*ATTN2*RF*RA*ATMDN*DISN*FUF*TRANS(FUT,PI1,RDISK,CI)
     1/D1/D1/D2/D2/FUT
      SUMNE=SUMNE+YLD*EN2
      SUMNTH=SUMNTH+YLD*THINC
      SUMD=SUMD+YLD
      YSCAT(INDEX)=YSCAT(INDEX)+YLD
      YSANG(JNDEX)=YSANG(JNDEX)+YLD
      YSEN(KNDEX)=YSEN(KNDEX)+YLD
  200 CØNTINUE
C
CXX   CØNTRIBUTIØN FRØM ØXYGEN ELASTIC SCATTERING
C
C     CALCULATE EN2,T2,INDEX AND KNDEX
C
  209 CALL KINAM(1.0067,15.995,1.0087,0.,EN1,THA,EN2,EDUM)
      KNDEX=EN2*FLØAT(NENR)/ENMAX
      KNDEX=KNDEX+1
      T2=TIME(EN2,D2)
      INDEX=(T1+T2-THIN)*FLØAT(NTIME)/TRANG
      INDEX=INDEX+1
      IF(INDEX.GT.NBIN) INDEX=NBIN
C
C     DETERMINE NØRMALIZED ØXYGEN DIFFERENTIAL ELASTIC SCATTERING
C     CRØSS SECTIØN
C
      CALL INTRPL(NØE,EØE,SIGØE,EN1,VSØE)
      DØ 211 I=1,5
      N=NWØE(I)
      DØ 210 J=1,N
      A(J)=EWØE(I,J)
  210 B(J)=WØE(I,J)
  211 CALL INTRPL(N,A,B,EN1,WØRK(I))
      CALL NØRM(WØRK,CØNST)
      CALL DISTR(5,WØRK,THA,S1)
      DESØ=CØNST*VSØE*S1*AVØG/PI2/2.0
C
C     CALCULATE ATTN2
C
      CALL INTRPL(NNT,ENT,SIGNT,EN2,VSNT)
      CALL INTRPL(NØT,EØT,SIGØT,EN2,VSØT)
      SIGAIR=AVØG*(ATMDN*VSNT+ATMDØ*VSØT)
      ATTN2=EXF(-SIGAIR*D2)
C
C     CALCULATE FUT AND FUF
C
      FUT=0.0
      DØ 221 I=1,4
      N=NUT(I)
      DØ 220 J=1,N
      A(J)=EUT(I,J)
  220 B(J)=SIGUT(I,J)
```

```
      CALL INTRPL(N,A,B,EN2,VSUT)
  221 FUT=FUT+ATMU(I)*VSUT
      FUT=FUT*AVØG
      FUF=0.0
      DØ 223 I=1,4
      N=NUF(I)
      DØ 222 J=1,N
      A(J)=EUF(I,J)
  222 B(J)=SIGUF(I,J)
      CALL INTRPL(N,A,B,EN2,VSUF)
  223 FUF=FUF+ATMU(I)*VSUF
      FUF=FUF*AVØG
C
      YLD=FS*CI*ATTN1*ATTN2*RF*RA*ATMDØ*DESØ*FUF*TRANS(FUT,PI1,RDISK,CI)
     1/D1/D1/D2/D2/FUT
      SUMNE=SUMNE+YLD*EN2
      SUMNTH=SUMNTH+YLD*THINC
      SUMD=SUMD+YLD
      YSCAT(INDEX)=YSCAT(INDEX)+YLD
      YSANG(JNDEX)=YSANG(JNDEX)+YLD
      YSEN(KNDEX)=YSEN(KNDEX)+YLD
C
CXX   CØNTRIBUTIØN FRØM ØXYGEN INELASTIC SCATTERING
C
      IF(MØI.EQ.0) GØ TØ 900
      DØ 300 IØI=1,MØI
C
C     CHECK IF REACTIØN IS ENERGETICALLY ALLØWED. CALCULATE T2,INDEX
C     AND KNDEX
C
      CALL KINAM(1.0087,15.995,1.0087,ØØI(IØI),EN1,THA,EN2,EDUM)
      IF(EN2) 300,300,290
  290 T2=TIME(EN2,D2)
      KNDEX=EN2*FLØAT(NENR)/ENMAX
      KNDEX=KNDEX+1
      INDEX=(T1+T2-TMIN)*FLØAT(NTIME)/TRANG
      INDEX=INDEX+1
      IF(INDEX.GT.NBIN) INDEX=NBIN
C
C     DETERMINE NØRMALIZED ØXYGEN DIFFERENTIAL INELASTIC SCATTERING
C     CRØSS SECTIØN (ISØTRØPIC)
C
      N=NØI(IØI)
      DØ 291 J=1,N
      A(J)=EØI(IØI,J)
  291 B(J)=SIGØI(IØI,J)
      CALL INTRPL(N,A,B,EN1,VSØI)
      DISØ=VSØI*AVØG/PI2/2.0
C
C     CALCULATE ATTN2
C
      CALL INTRPL(NNT,ENT,SIGNT,EN2,VSNT)
      CALL INTRPL(NØT,EØT,SIGØT,EN2,VSØT)
      SIGAIR=AVØG*(ATMØN*VSNT+ATMØØ*VSØT)
      ATTN2=EXF(-SIGAIR*D2)
C
C     CALCULATE FUT AND FUF
C
      FUT=0.0
      DØ 293 I=1,4
```

```
      N=NUT(I)
      DØ 292 J=1,N
      A(J)=EUT(I,J)
  292 B(J)=SIGUT(I,J)
      CALL INTRPL(N,A,B,EN2,VSUT)
  293 FUT=FUT+ATMU(I)*VSUT
      FUT=FUT*AVØG
      FUF=0.0
      DØ 295 I=1,4
      N=NUF(I)
      DØ 294 J=1,N
      A(J)=EUF(I,J)
  294 B(J)=SIGUF(I,J)
      CALL INTRPL(N,A,B,EN2,VSUF)
  295 FUF=FUF+ATMU(I)*VSUF
      FUF=FUF*AVØG
C
      YLD=FS*CI*ATTN1*ATTN2*RF*RA*ATMDØ*DISØ*FUF*TRANS(FUT,PI1,RDISK,CI)
     1/D1/D1/D2/D2/FUT
      SUMNE=SUMNE+YLD*EN2
      SUMNTH=SUMNTH+YLD*THINC
      SUMD=SUMD+YLD
      YSCAT(INDEX)=YSCAT(INDEX)+YLD
      YSANG(JNDEX)=YSANG(JNDEX)+YLD
      YSEN(KNDEX)=YSEN(KNDEX)+YLD
  800 CØNTINUE
C
  900 CØNTINUE
      CALL SSWTCH(1,K1)
      IF(K1.EQ.1) GØ TØ 905
      IF(NHIST-NHISTL) 113,905,905
C
C.....
C
C     CALCULATE HISTØRY AVERAGES AND MULTIPLY BY AIR PARAMETER SPACE
C     VØLUME
C
  905 VØLU=2.0*RAMAX*ZAMAX*PI2
      DØ 906 I=1,NANG
  906 YSANG(I)=VØLU*YSANG(I)/FLØAT(NHIST)
      DØ 907 I=1,NENR
  907 YSEN(I)=VØLU*YSEN(I)/FLØAT(NHIST)
      DØ 910 I=1,NBIN
  910 YSCAT(I)=VØLU*YSCAT(I)/FLØAT(NHIST)
C
C     CALCULATE RATIØ(I),RANG(I),REN(I),TØTRAT,FT1 AND FT2
C
      TØTRAT=0.0
      DØ 1000 I=1,NBIN
      RATIØ(I)=YSCAT(I)/YDIR
 1000 TØTRAT=TØTRAT+RATIØ(I)
      DØ 1001 I=1,NANG
 1001 RANG(I)=YSANG(I)/YDIR
      DØ 1002 I=1,NENR
 1002 REN(I)=YSEN(I)/YDIR
      FT2=RATIØ(NBIN)/TØTRAT
      FT1=1.0-FT2
C
C     CALCULATE AVERAGE EN2 AND THINC
C
```

```
      EN2V=SUMNE/SUMD
      THINCV=SUMNTH/SUMD
C
C     WRITE RESULTS
C
      WRITE(5,1900) YDIR
 1900 FØRMAT(4HYDIR/E10.4)
      WRITE(5,2000) TMIN,DT,FREE
 2000 FØRMAT(12HTMIN,DT,FREE/3E10.4)
      WRITE(5,2020) NHIST
 2020 FØRMAT(8HNHIST = ,I6)
      WRITE(5,4000)
 4000 FØRMAT(7HENER(I))
      WRITE(5,3000) (ENER(I),I=1,NENR)
      WRITE(5,4001)
 4001 FØRMAT(6HREN(I))
      WRITE(5,3000) (REN(I),I=1,NENR)
      WRITE(5,4002)
 4002 FØRMAT(7HTHIC(I))
      WRITE(5,3000) (THIC(I),I=1,NANG)
      WRITE(5,4003)
 4003 FØRMAT(7HRANG(I))
      WRITE(5,3000) (RANG(I),I=1,NANG)
      WRITE(5,2001)
 2001 FØRMAT(4HT(I))
      WRITE(5,3000) (T(I),I=1,NTIME)
 3000 FØRMAT(4E10.4)
      WRITE(5,2002)
 2002 FØRMAT(8HRATIØ(I))
      WRITE(5,3000) (RATIØ(I),I=1,NBIN)
      WRITE(5,2003) TØTRAT,FT1,FT2
 2003 FØRMAT(14HTØTRAT,FT1,FT2/3E10.4)
      WRITE(5,2004) EN2V,THINCV
 2004 FØRMAT(11HEN2V,THINCV/2E10.4)
      WRITE(5,2005)
 2005 FØRMAT(/5H-----)
C
      IF(K1.EQ.1) PAUSE
      GØ TØ 1
      END
      FUNCTIØN TIME(EIN,R)
      E=EIN/939.549
      IF(E.GT.0.) GØ TØ 1
      V=0.0
      GØ TØ 2
    1 V=(+.2997925E+11)*SQRT(ABS(1.0-(1.0/(E+1.0)/(E+1.0))))
      TIME=R/V
    2 RETURN
      END
      SUBRØUTINE KINAM(A1,A2,A3,Q,E1,TH3,E31,E32)
C
      W1=931.478*A1
      W2=931.478*A2
      W3=931.478*A3
      W4=W1+W2-W3-Q
      EF=-Q*(1.0+(W1/W2)-(0.5*Q/W2))
      EB=-Q*(1.0+(W1/(W2-W3))-(0.5*Q/(W2-W3)))
      IF(E1-EF) 1,1,2
    1 E31=0.0
   11 E32=0.0
```

```
      GØ TØ 6
    2 C=CØS(TH3)
      A=2.0*(W3+W4+E1+Q)
      B=2.0*E1*(W1-W4-Q)-(2.0*W4*Q+Q*Q)
      D=E1*(E1+2.0*W1)*C*C
      TERM=(B*B-2.0*W3*A*B+4.0*W3*W3*D)*E1*(E1+2.0*W1)
      IF(TERM) 1,1,3
    3 DEN=A*A-4.0*D
      U=(4.0*W3*D-A*B)/DEN
      V=2.0*C*SQRT(ABS(TERM))/DEN
      E31=U+V
      IF(E1-EB) 4,4,5
    4 IF(TH3-1.5707963) 41,11,11
   41 E32=U-V
      GØ TØ 6
    5 E32=E31
    6 RETURN
      END
      SUBRØUTINE ANGLE(X1H,Y1H,Z1H,X1T,Y1T,Z1T,X2H,Y2H,Z2H,X2T,Y2T,Z2T,T
     1H)
      V1=SQRT(ABS((X1H-X1T)*(X1H-X1T)+(Y1H-Y1T)*(Y1H-Y1T)+(Z1H-Z1T)*(Z1H
     1-Z1T)))
      V2=SQRT(ABS((X2H-X2T)*(X2H-X2T)+(Y2H-Y2T)*(Y2H-Y2T)+(Z2H-Z2T)*(Z2H
     1-Z2T)))
      DØT=(X1H-X1T)*(X2H-X2T)+(Y1H-Y1T)*(Y2H-Y2T)+(Z1H-Z1T)*(Z2H-Z2T)
      CTH=DØT/V1/V2
      TH=ARCCØS(CTH,2)
      RETURN
      END
      SUBRØUTINE NØRM(W,C)
      DIMENSIØN W(5)
      SUM=0.0
      DØ 1 I=1,36
      TH=3.14159*FLOAT(I)/36.0
      CALL DISTR(5,W,TH,S)
    1 SUM=SUM+S*SIN(TH)
      SUM=0.0872664*SUM
      C=2.0/SUM
      RETURN
      END
      SUBRØUTINE DISTR(NW,W,TH,V)
      DIMENSIØN W(5)
      V=1.0
      IF(NW.EQ.0) GØ TØ 4
      DØ 2 I=1,NW
    2 V=V+W(I)*PØLYL(2,I,TH)
      IF(V) 3,4,4
    3 V=0.0
    4 RETURN
      END
      FUNCTIØN PØLYL(IØP,N,ANGLE)
      X = ANGLE
      GØ TØ(10,11,12),IØP
   10 X = .017453293*X
   11 X = CØS(X)
   12 NBIG = N-1
      IF(NBIG) 1,2,3
    1 PØLYL = 1.0
      GØ TØ 100
    2 PØLYL = X
```

```
      GØ TØ 100
    3 PL = X
      PLM1 = 1.0
      DØ 4 L=1,NBIG
      PØLYL = (FLØAT(2*L+1)*X*PL - FLØAT(L)*PLM1)/FLØAT(L+1)
      PLM1 = PL
    4 PL = PØLYL
  100 RETURN
      END
      SUBRØUTINE INTRPL(N,XT,YT,X,Y)
      DIMENSIØN XT(N),YT(N)
      IF(X-XT(1)) 1,3,4
    1 WRITE(1,2)
    2 FØRMAT(8HRANG ERR)
      PAUSE
    3 Y=YT(1)
      GØ TØ 24
    4 IF(X-XT(N)) 7,5,1
    5 Y=YT(N)
      GØ TØ 24
    7 I=0
      J=N
    8 K=0.5*FLØAT(J-I)+0.1
      K=K+I
      IF(X-XT(K)) 9,10,11
    9 J=K
      GØ TØ 12
   10 Y=YT(K)
      GØ TØ 24
   11 I=K
   12 IF(J-I-1) 13,13,8
   13 I=J
      J=I-1
      DEN=XT(J)-XT(I)
      C1=(XT(J)*YT(I)-XT(I)*YT(J))/DEN
      C2=(YT(J)-YT(I))/DEN
      Y=C1+C2*X
   24 RETURN
      END
      FUNCTIØN ARCCØS(X,K)
      ARCCØS=1.5707963
      IF(ABS(X).GT..999999) X=.999999*X/ABS(X)
      IF(X*X.GT.1.0E-70) ARCCØS=ATAN(SQRT(ABS(1./X/X-1.)))
      IF(X.LT.0.) ARCCØS=3.1415926-ARCCØS
      GØ TØ (100,200),K
  100 ARCCØS=ARCCØS*57.2957795
  200 RETURN
      END
      FUNCTIØN TRANS(F,P,R,C)
      V=F/P/R/R/C
      IF(V-0.001) 1,1,2
    1 TRANS=V-(0.5*V*V)
      GØ TØ 3
    2 TRANS=1.0-EXF(-V)
    3 RETURN
      END
      FUNCTIØN EXF(Z)
      IF(Z) 1,1,3
    1 IF(Z.LT.-70.0) Z=-70.0
      IF(Z.GT.-.1E-04) GØ TØ 2
```

```
      EXF=EXP(Z)
      GØ TØ 4
    3 IF(Z.GT.70.0) Z=70.0
      IF(Z.LT..1E-04) GØ TØ 2
      EXF=EXP(Z)
      GØ TØ 4
    2 EXF=1.0+Z
    4 CØNTINUE
      RETURN
      END
$
```